Finite Element Modeling of the Human Head

Svein Kleiven
Department of Aeronautics
Royal Institute of Technology
S-100 44 Stockholm, Sweden

Report 2002 – 9
ISSN 0280-4646

Academic dissertation which with permission from Kungliga Tekniska Högskolan (Royal Institute of Technology) in Stockholm is presented for public review for passing the doctoral examination 10.15 am Wednesday 29th of May 2002 in Kollegiesalen, KTH, Valhallavägen 79, Stockholm, Sweden.

Til min mor

Preface

The work presented in this Doctoral Thesis has been carried out at the Department of Aeronautics, the Royal Institute of Technology, between 1998 and 2002. I want to acknowledge the Swedish Transport & Communications Research Board for providing the financial support for this work.

I want to thank my dear colleague Peter Halldin at the Department of Aeronautics, KTH, for being such a nice and helpful room-mate, as well as, together with my two other colleagues at the Neuronics; Karin Brolin and Magnus Aare, for open minded and stimulating discussions. I am grateful to Professor Jan Bäcklund, head of the Department, for his enthusiasm. I want to thank the Engineering Research AB for providing me with excellent software and assistance. Especially acknowledged for all support with ls-dyna are Ragnar Lindström, Åsa Gökstorp, and Daniel Hilding. I would like to express my sincere gratitude to my supervisor, Professor Hans von Holst, who really is a source of optimism, encouragement, fruitful ideas and support. Thank you, Hans! My gratitude to all the supportive colleagues at the Department, which have greatly facilitated my work.

For my beloved Silvia I don't have enough words, so I simply say ¡Te quiero!

Stockholm, April 2002

Svein Kleiven

Abstract

The main objectives of the present thesis were to define the dimension of head injuries in Sweden over a longer period and to present a Finite Element (FE) model of the human head which can be used for preventive strategies in the future. The annual incidence of head injuries in Sweden between 1987 and 2000 was defined at over 22 000, cases most of which were mild head injuries. In contrast to traffic accidents, head injuriy due to fall was the most important etiology. Of special interest was that the number of hematoma cases has increased.

A detailed and parameterized FE model of the human head was developed and used to evaluate the effects of head size, brain size and impact directions. The maximal effective stresses in the brain increased more than a fourfold, from 3.6 kPa for the smallest head size to 16.3 kPa for the largest head size using the same acceleration impulse. The size dependence of the intracranial stresses associated with injury is not predicted by the Head Injury Criterion (HIC).

Simulations with various brain sizes indicated that the increased risk of Subdural Hematoma (SDH) in elderly people may to a part be explained by the reduced brain size resulting in a larger relative motion between the skull and the brain with distension of bridging veins. The consequences of this increased relative motion due to brain atrophy cannot be predicted by existing injury criteria.

From studies of the influence of impact directions to the human head, the highest shear strain in the brain stem is found for a Superior-Inferior (SI) translational impulse, and in the corpus callosum for a lateral rotational impulse when imposing acceleration pulses corresponding to the same impact power. It was concluded that HIC is unable to predict consequences of a pure rotational impulse, while the Head Impact Power (HIP) criterion needs individual scaling coefficients for the different terms to account for differences in intracranial response due to a variation in load direction. It is also suggested that a further evaluation of synergic effects of the directional terms of the HIP is necessary to include combined terms and to improve the injury prediction.

Comparison of the model with experiments on localized motion of the brain shows that the magnitude and characteristics of the deformation are highly sensitive to the shear properties of the brain tissue. The results suggest that significantly lower values of these properties of the human brain than utilized in most 3D FE models today must be used to be able to predict the localised brain response of an impact to the human head. There is a symmetry in the motion of the superior and inferior markers for both the model and the experiments following a sagittal and a coronal impact. This can possibly be explained by the nearly incompressible properties of brain tissue. Larger relative motion between the skull and the brain is more apparent for an occipital impact than for a frontal one in both experiments and FE model. This correlates with clinical findings. Moreover, smaller relative motion between the skull and the brain is more apparent for a lateral impact than for a frontal one for both experiments and FE model. This is thought to be due to the supporting structure of the falx cerebri.

Such a parametrized and detailed 3D model of the human head has not, to the best knowledge of the author, previously been developed. This 3D model is thought to be of significant value for looking into the effects of geometrical variations of the human head.

Dissertation

This Doctoral Thesis presents an overview of the research in the area of Finite Element Modeling of the human head and includes the following papers:

Paper A

Svein Kleiven, Paul M. Peloso, Hans von Holst (2002). The Epidemiology of Head Injuries in Sweden From 1987 to 2000. *Submitted to Journal of Injury Control and Safety Promotion.*

Paper B

Svein Kleiven, Hans von Holst (2002). Consequences of head size following trauma to the human head. *Journal of Biomechanics* **35** (2), 153 – 160.

Paper C

Svein Kleiven, Hans von Holst (2002). Consequences of Brain Volume following Impact in Prediction of Subdural Hematoma evaluated with Numerical Techniques. *Accepted for publication in Traffic Injury Prevention.*

Paper D

Svein Kleiven (2001). Influence of Impact Direction to the Human Head in Evaluation of Head Injury Criteria: A Numerical Study. *Submitted to Journal of Neurotrauma.*

Paper E

Svein Kleiven, Warren N. Hardy (2002). Correlation of an FE model of the Human Head with Experiments on localized Motion of the Brain – Consequences for Injury Prediction. *Manuscript.*

Division of Work Between Authors

Paper A

Kleiven analyzed the epidemiological data, and extracted the results. Von Holst initiated the work, and assisted in the data analysis. Peloso provided additional comments.

Paper B and C

Kleiven performed the analysis and wrote the papers under von Holsts supervision.

Paper E

Hardy performed the coronal plane experiment. The sagittal plane experiments was also performed by Hardy with assistance of Kleiven. Kleiven initiated the numerical study, performed the analysis, and wrote the paper with additional commentaries by Hardy.

Table of Contents

PREFACE i

ABSTRACT iii

DISSERTATION v

DIVISION OF WORK BETWEEN AUTHORS vii

TABLE OF CONTENTS ix

1 INTRODUCTION 1

1.1 Background 1

1.2 Scope of the investigation 2

1.3 Anatomy of the Human Head 2

1.4 Material Properties of the Human Head 3

1.5 Brain injury mechanisms 11

1.6 Head Injury Criteria 13

1.7 Review of Finite Element Models of the Human Head 19

1.8 Review of Studies regarding Head, and Brain Size 25

1.9 Review of Studies regarding Head Kinematics 26

2 NUMERICAL METHODS 30

2.1 Theory of Explicit Finite Element Programs 30

2.2 Time integration 31

2.3 Mooney-Rivlin Hyperelasticity for Brain Tissue 32

3 DISCUSSION 34

4 CONCLUSIONS 38

5 FUTURE WORK 40

REFERENCES 41

Paper A A1-A11

Paper B B1-B8

Paper C C1-C13

Paper D D1-D15

Paper E E1-E19

1 Introduction

1.1 Background

Neurotrauma is the physical damage that results when the human skull and brain are suddenly or briefly subjected to intolerable levels of energy that is usually transmitted mechanically. An injury to the central nervous system is the most serious type of traumatic injury. The causes of neurotrauma are well established and include traffic accidents, falls, assaults and injuries occurring during recreational or sports activities.

Most of the research in the injury prevention area was initiated by the military aircraft industry in the sixties and seventies. Today the research is to a greater extent sponsored by the car manufacturing industry, partly as a result of the demands from the customers and the media.

Current trends suggest an increase in the number of survivors of neurotrauma throughout the world. This demands a new outlook giving high priority to establishing long-term goals in preventing, treating and rehabilitating people with an injury to the central nervous system. However, the exact percentage of deaths with significant brain injury is not known although it can be estimated using several published parameters. Worldwide brain injury mortality rates range from about 15 to 30 per 100 000 population annually. If a mean mortality rate of 22 per 100 000 is applied to the world population of 6 billion people, approximately 1.2 million are found to die annually with associated traumatic brain injury. In other words, from 5 to 10 percent of all deaths are related to trauma and approximately 40 percent of these are due to traumatic brain injury.

Another measure of impact of brain trauma in society is the case fatality rate, that is, the proportion of deaths among those hospitalized with traumatic brain injury. There is considerable variation worldwide, probably representing different policies for hospitalization. Nevertheless, somewhere between 5 and 10 percent of all those admitted to a hospital die during their stay from traumatic brain injury.

Counts of the number and rate of hospitalized admissions are not known. However, there are indications that approximately 150 per 100 000 persons are discharged from hospitals following traumatic brain injury observation or treatment. In developed countries the fatality ratio for persons admitted to emergency rooms for traumatic brain injury ranges from approximately 1:7 to 56. That is, for each fatality there are approximately 7 individuals hospitalized and 56 persons examined, treated and released from care for traumatic brain injury. However, the exact number of traumatic brain injuries is not known, since many countries worldwide lack an adequate injury surveillance system for traumatic brain injuries.

The pathophysiological mechanisms following neurotrauma have, to some extent, been elucidated during the last decade. Neurotrauma is not a single event but a cascade of neuromechanical and neurochemical consequences. Health care providers have becomed increasingly aware of these injuries, not as ”all or nothing” events, but as time-dependent events evolving during the minutes, hours and days following the injury. Even though the medical consequences today remain serious in many cases, current research in neurotrauma is creating optimism for future medical treatment that may substantially reduce complications now seen

following injury to the central nervous system. However, there is a long way to go before a complete understanding of the pathophysiological events following an accident is reached.

The introduction of new imaging techniques such as magnetic resonance imaging has increased the knowledge and treatment efficacy following traumatic brain injury. Further development of three-dimensional techniques will improve the medical treatment and outcome substantially due to better understanding of what happens at the scene of the accident.

1.2 Scope of the investigation

This study primarily focuses on the development of a 3D FE model of the Human Head.

The present thesis includes:

- The evaluation of incidence rate of head injuries in Sweden between 1987 and 2000.
- The development of a parameterized 3D Finite Element (FE) model of the human head.
- Parametric studies of the influences of head and brain size for intracranial responses of an impact.
- Evaluation of the intracranial responses to a variation of impact direction to the human head, and its consequences for injury prediction.
- Experimental validation of the FE model against recently presented experiments on localized brain motion, utilizing different stiffness properties of the brain tissue, and various techniques for modeling the skull-brain interface of the human head.

1.3 Anatomy of the Human Head

Different tissue layers such as the scalp, skull bone, dural, arachnoidal and pial membranes as well as cerebrospinal fluid (CSF) cover the brain. (Fig. 1). The skullbone can be viewed as a three-layered sandwich structure with an inner and outer table of compact bone and a diploë of spongy bone sandwiched between them as a core. A sagittal dural partition membrane, the falx cerebri, partly separates the left and right hemispheres of the brain (Fig. 4). The lower separating membrane, the tentorium cerebelli, resides on the inferior wall of the skull, and separates the cerebrum from the cerebellum and brain stem. The brain, with its covering membranes and CSF, is connected to the spinal cord through the foramen magnum. The inferior part of the skull base is attached to the neck by articulation through occipital condyles, ligaments and muscles.

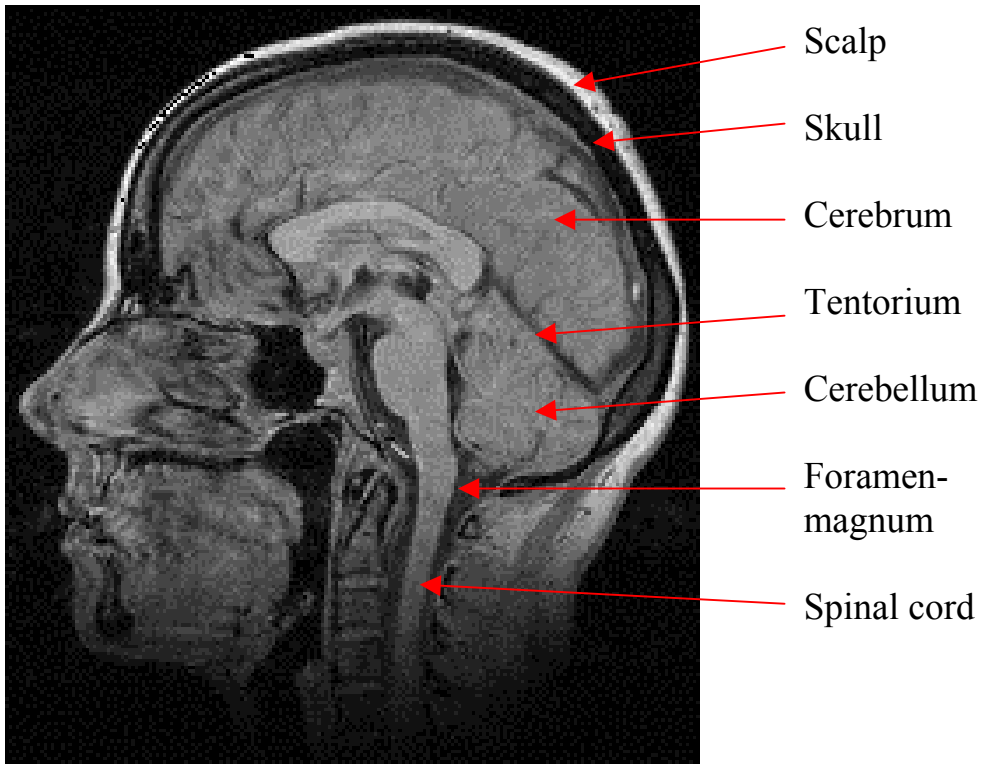

Figure 1 – CT scan of a sagittal section of the human head.

1.4 Material Properties of the Human Head

Biological materials do not follow the constitutive relations for common engineering materials. A biological material is often anisotropic, inhomogeneous, nonlinear and viscoelastic. In addition, there is a great variability between different individuals.

Scalp

The scalp is 5 to 7 mm thick and consists of three layers: the hair-bearing skin (cutaneous layer), a subcutaneous connective tissue layer, and a muscle and facial layer. Beneath the scalp there is a loose connective layer plus the fibrous membrane that covers the bones.

A limited number of fresh human scalp specimens were tested in compression by Melvin *et al.* (1970). The material behaviour is almost linearly elastic until strains of 30-40 % were applied. Larger strains give a concave stress-strain curve which is typical of most soft biological tissues.

A series of relaxation tests were performed in tension on monkey scalp specimens (Galford and McElhaney, 1970). The specimen was brought to an instantaneous fixed strain and the load was measured over a period of time. A typical viscoelastic stress relaxation behavior for the monkey scalp was seen.

Cranial bones

The thickness of the skull varies between 4 and 7 mm. The base of the braincase is an irregular plate of bone containing depressions and ridges plus small holes (foramen) for arteries, veins, and nerves, as well as the large hole (the foramen magnum) that is the transition area between the spinal cord and the brainstem (Fig. 2). The bones of the cranium are connected at lines called sutures.

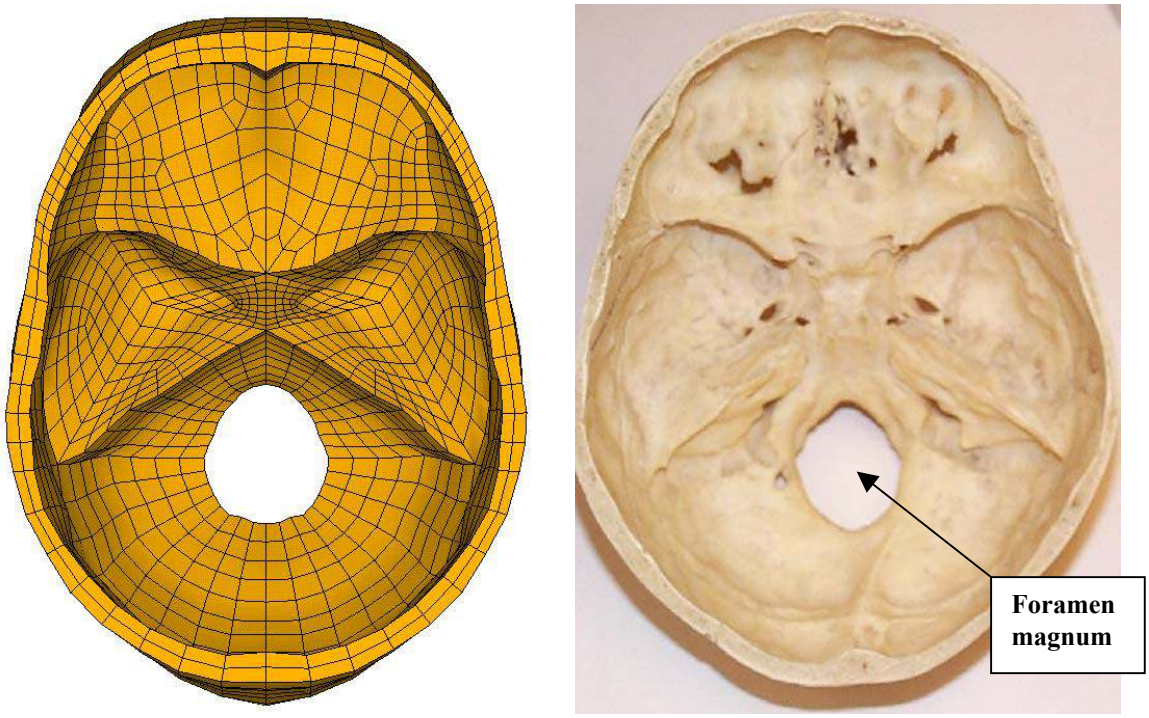

Figure 2 – Skullbase of the human head (right), and an FE representation of the skullbase using an intermediate element mesh density (left).

Several experiments have been performed on human cranial bones. The bones considered in the experiments were the frontal, left and right parietal, and the occipital (Fig 3). In the human, these bones show two well-defined shells of compact bones separated by a core of spongy cancellous bone, called diploë. Compact bone surrounds and reinforces the sutures. The inner and outer layer of compact bone in the skull can (unlike the long bones) be considered to be isotropic in the tangential direction of the skull bone (transversely isotropic).

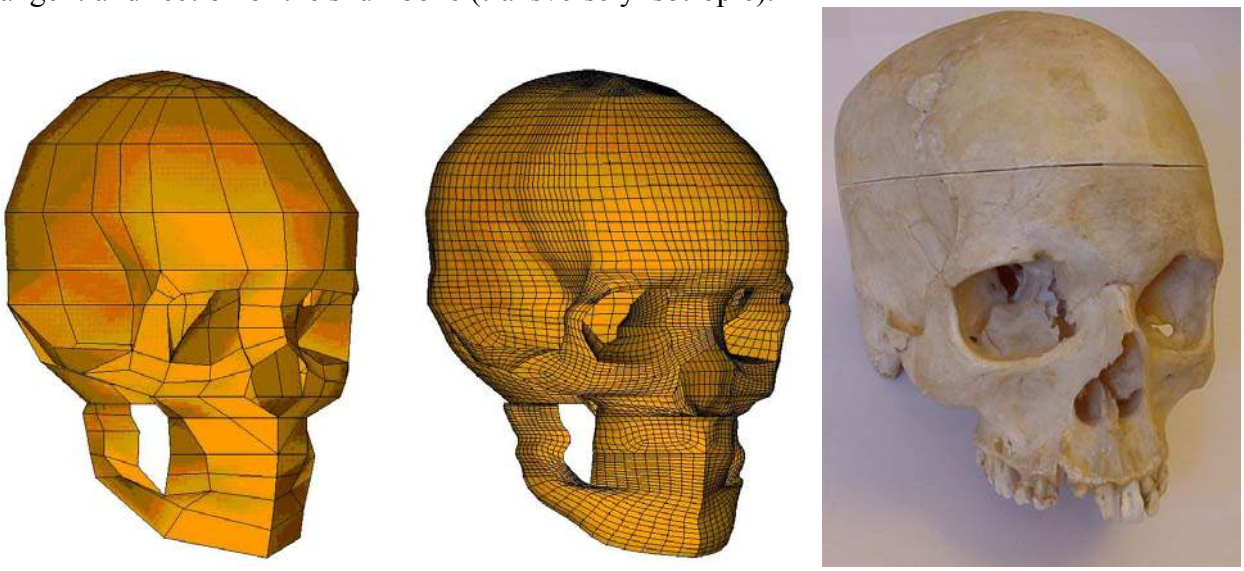

Figure 3 – Cranial bones of the human head (right), and an FE representation of the cranial bones with a coarse element mesh (left), and a refined mesh (middle).

This can be explained by the random orientation of the cortical grain structure of the inner and outer table of compact bone. The spongy bone is quite variable in structure with marrow spaces normally ranging from 3 mm in diameter down to microscopic size. This gives a wide range of mechanical responses. In a series of experiments performed on human cranial bones (McElhaney

et al., 1970), the modulus of elasticity for tangential compression was found to be more than 2 times larger than that for radial compression. By compression tests, and measurement of the deformation in both the load direction and perpendicular to it the Poisson's ratio was determined for both the radial direction, $v_r=0.19$, and the tangential direction, $v_t=0.22$.

A summary of the properties of the cranial bone determined in different studies can be seen in Table 1. Below. In a recent study performed by Schueler *et al.* (1994), specimens with quadratic surfaces and a large width and length ratio compared to the height were used. The large aspect ratio has been shown to give errors due to increased influence of the friction in the surfaces between specimen and loading fixture. For testing of cellular materials, cylindrical specimens should be used, aiming at a homogeneous deformation. Vrijhoef and Driessens (1971) estimated the optimal length-diameter ratio for an isotropic homogeneous specimen under compression in order to avoid buckling, and in order to minimize the effect of frictional restraint at the compression platen. They found the range of acceptable L/D ratios to be 1-5 and suggested an L/D ratio of 2 as the optimal geometry.

Table 1 – Properties of cranial bone.

Reference	***Ec*** *GPa*	σ_{fc} *MPa*	***Et*** *GPa*	σ_{ft} *MPa*	τ_{fd} *MPa*
McElhaney *et al.* (1970)	2.4*	73.8	12.4-20.0#	69.0-98.6#	21.4
Barber *et al* . (1970)	0.7	71.5			
Melvin *et al* . (1970)	1.0	32.4			
Robbins *et al.* (1969)	1.4	36.6	14.6	65.5	13.1
Wood (1971)			10.3-22.1#	48.3-127.6#	
Schueler *et al.* (1994)	0.3	130.0			15.0

E_c=Young's modulus in radial compression, σ_{fc}=failure stress in radial compression, E_t=Young's modulus for compact bone in tension, σ_{ft}=failure stress for compact bone in tension, τ_{fd}=failure stress for diploë in shear.

*Results from very porous diploë were removed from the analysis.
#Young's modulus and failure stress depends on strain rate.

Strain rate sensitivity
In order to determine the strain rate sensitivity of human cranial bone, researchers (Wood, 1971, and McElhaney *et al.*, 1970) conducted tensile experiments on specimens taken from the compact layers of the parietal, temporal and frontal bones. The results of the experiments performed by Wood (1971) showed that the modulus of elasticity increases with the strain rate. In the same way, the failure stress increases with the strain rate while the ultimate strain decreases with the strain rate.

Meninges
The meninges consist primarily of connective tissue, and they also form part of the walls of blood vessels and the sheaths of nerves as they enter the brain and as they emerge from the skull. The meninges consists of three layers: the dura mater, the arachnoid, and the pia mater.

Brain tissue, having the consistency of a heavy pudding, is the most delicate of all body tissues. For protection, this vital organ is located in a sealed bony chamber, the skull. To protect it further from the rough bone and from blows and shocks to the head, the brain is enveloped by the meninges. The outermost dura mater is adherent or close to the inner surface of the bone (Fig. 4). Beneath the dura mater is the middle covering, the thin and fibrous arachnoid. The third and innermost layer is the very thin, delicate, and capillary-rich pia-mater, which is intimately attached to the brain and dips down into the sulci and fissures.

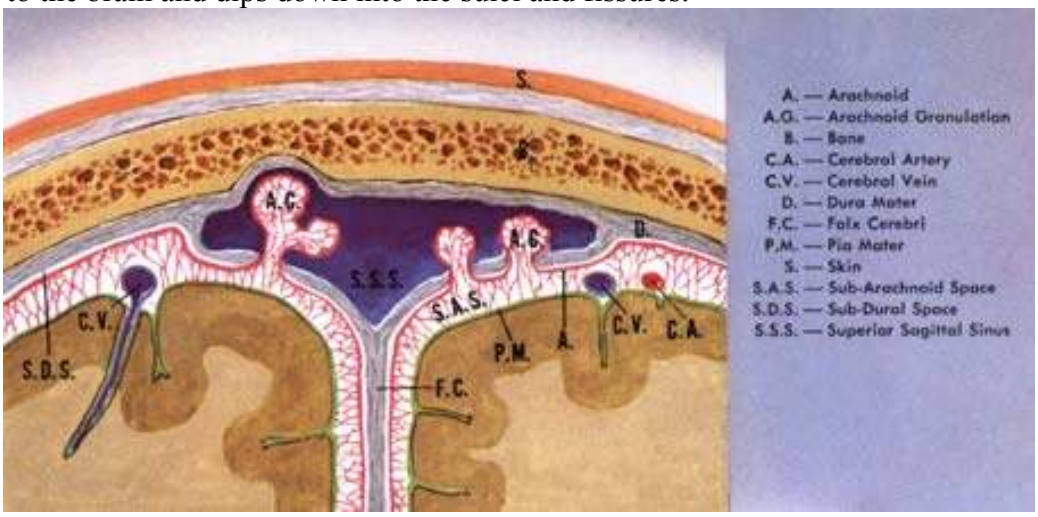

Figure 4 – The meningeal membranes in a coronal cross section, from a frontal view point.

Between the dura mater and the underlying arachnoid is a narrow subdural space filled with a small amount of fluid that acts as a lubricant, preventing adhesion between the two membranes. Separating the arachnoid from the pia mater is a relatively large gap, the subarachnoid space, which is filled with CSF (Fig. 4). This clear, lymphlike fluid fills the entire subarachnoid space and surrounds the brain with a protective cushion that absorbs shock waves to the head. As a further means of protection, there are fibrous filaments known as arachnoid trabeculations, which extend from the arachnoid to the pia and help "anchor" the brain to prevent it from excessive movement in cases of sudden acceleration or deceleration.

Very few experiments have been carried out on human meningeal tissues. Only reports regarding the properties of dura mater have been found and reviewed.

Dura Mater

The dura mater is a tough, fibrous membrane that surrounds the spinal cord and the inner surface of the skull. Folds of the dura mater form the falx cerebri, which projects into the longitudinal fissure between the right and left cerebral hemispheres (Fig. 4 and 5). Another dural fold forms the tentorium cerebelli (Fig. 5), a membrane separating the cerebrum from the cerebellum and brain stem.

The Young's modulus of human dura mater was determined using tensile testing by Melvin *et al.* (1970). Following dissection, they stated that the macrostructure of the dura mater appeared to be a membrane with evident directions of fiber reinforcement. However, strain rate effects and biological variability overshadowed the effect of the fiber direction. They found values in the range of 41-55 *MPa* for the Young's modulus in tension. The results showed that a small amount of initial strain occurs with no load. This can be explained by the fibrous tissue not taking any

load during small deformations. It just straightens out, and only the weaker connective tissue takes load.

Tensile creep tests were performed by Galford and McElhaney (1970) on human and monkey dura mater to derive viscoelastic parameters. An ideal creep experiment consists of measuring the deformation-time history of a material sample subjected to a constant stress. The creep compliance curves are linear on a semilog graph. The ultimate strain for dura mater has been determined to lie between 0.130 and 0.181 and the strength to lie between 1.44 and 4.65 *MPa* in tension by Zhivoderov *et al.* (1982).

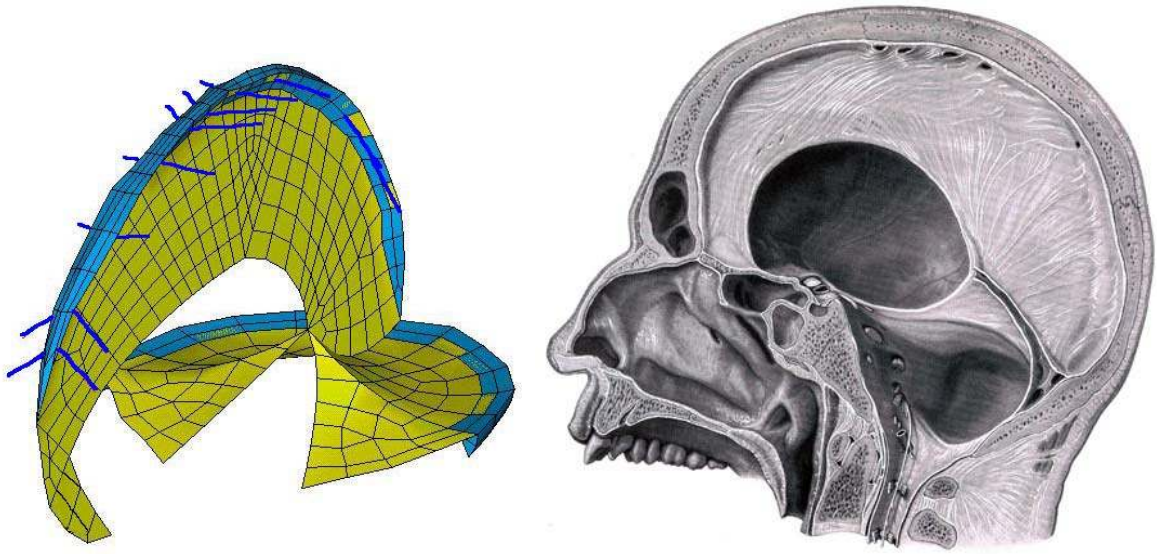

Figure 5 – The internal, separating membranes; *tentorium* and *falx* of the human head (right*). An FE representation of the falx and tentorium, including the super sagittal and transverse sinuses and eleven pairs of the bridging veins (left).

Brain Tissue

At a microscopic level, the Central Nervous System (CNS) is primarily a network of neurons and supportive tissue functionally arranged into areas that are gray or white in color. Gray matter is composed primarily of nerve-cell bodies concentrated in locations on the surface of the brain and deep within the brain. White matter is composed of myelinated (myelin=a soft white somewhat fatty material) axons that largely form tracts to connect parts of the CNS to each other.

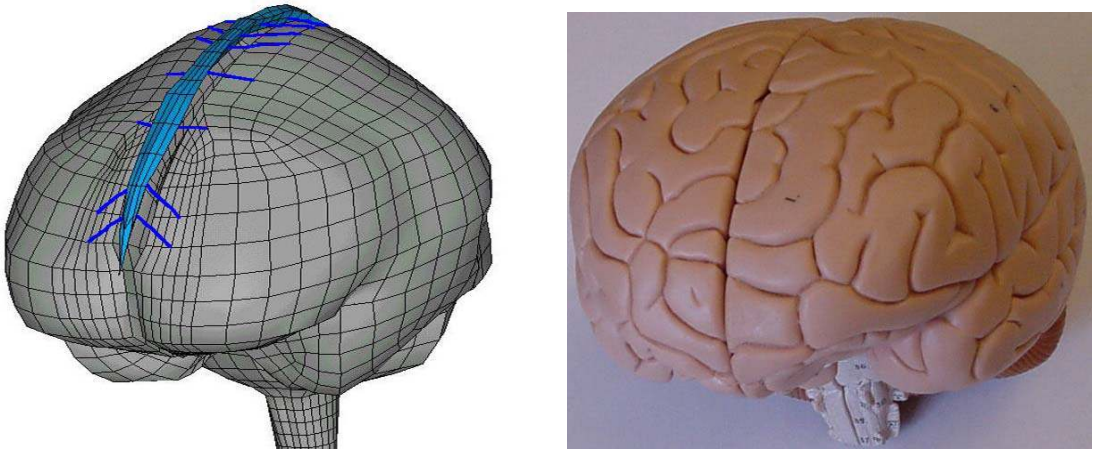

Figure 6 – The brain.

From the standpoint of engineering material, brain tissue can be likened to a soft gel. Because of the high water content (about 80 %), it is nearly incompressible. This is also confirmed by

reported values of the bulk modulus for brain tissue of about K=2.1 *GPa* (Stalnaker, 1969, McElhaney *et al.*, 1976) which is roughly 10^5 times larger than the shear modulus. Thus, the deformation of brain tissue can be assumed to depend on the shear modulus only. Most of the testing of brain tissue has therefore been performed in shear or torsion.

Complex Modulus

The simplest way to determine the viscoelastic properties of soft biological tissues is to subject the material to periodic oscillations, due to the consistency and problems with load introduction. Briefly, a specimen is sandwiched between two parallel plates constructed of roughened glass coverslips. The bottom plate is attached to a linear bearing and the top plate is fixed. The linear actuator is driven sinusoidally with a specified amplitude and frequency. The displacement of the bottom plate is measured while the force transmitted through the sample is measured by a force transducer attached to the top plate. From these measurements, the complex shear modulus, $|G^*| = \sqrt{G'^2 + G''^2}$, can be calculated at steady state using the following formulas:

$$G' = \left(\frac{\tau_0}{\gamma_0}\right)\cos(\delta) \quad \text{and} \quad G'' = \left(\frac{\tau_0}{\gamma_0}\right)\sin(\delta)$$

Where τ_0 and γ_0 are the amplitudes of the sinusoidally varying shear stress and shear strain, respectively, and δ is the phase difference between the two signals.

The complex dynamic shear modulus, G^* of a viscoelastic material is defined as the vector sum of G' and iG'', with G'' normal to G':

$$G^* = G' + iG''$$

G' is a measure of the spring stiffness of the test material under shear, and is called the storage modulus. The dynamic loss modulus, G'', is a measure of the damping ability of the material and represents viscous stresses in the material.

Directional Properties & Regional Differences

The directional properties of human gray and white brain tissue were tested in torsion (Shuck and Advani, 1972). The purpose of these tests was to determine if the material could be considered macroscopically isotropic. From the tests it appeared that white matter may be considered isotropic for engineering purposes. However, gray matter, showed variations in the storage modulus for each of the axes and was also different from white matter. The loss modulus showed small variations both for white and gray matter. Although the properties for gray matter show directional preference and differ from those of white matter, they concluded that the differences could be considered small. More recent studies on pig brain (Arbogast *et al.*, 1997) concluded that white matter is stiffer than gray matter, by comparing the instantaneous elastic moduli. These were found to be: G_0^{white}=1036 *kPa* and G_0^{gray}=681 *kPa*. This difference can be explained by the fibrous nature of white matter. The same researchers also did a study of the regional differences (on pig brain), and found that in oscillating shear tests the complex modulus of the brainstem was about 80% greater than for the cerebrum. Later research (Prange *et al.*, 2000) reported that gray matter is only slightly (about 4 %) stiffer than white matter when utilizing large strains in simple shear. This illustrates some of the difficulties in determining the properties for brain tissue, as well as the implementation in a numerical model.

Strain rate sensitivity

As seen from the typical stress-strain curves for brain tissue in simple shear (Fig.7), the stiffness increases with the strain, i.e. the stress-strain curves are concave. Further, it can be seen that the stiffness increases with the strain rate (Donnelly and Medige, 1997).

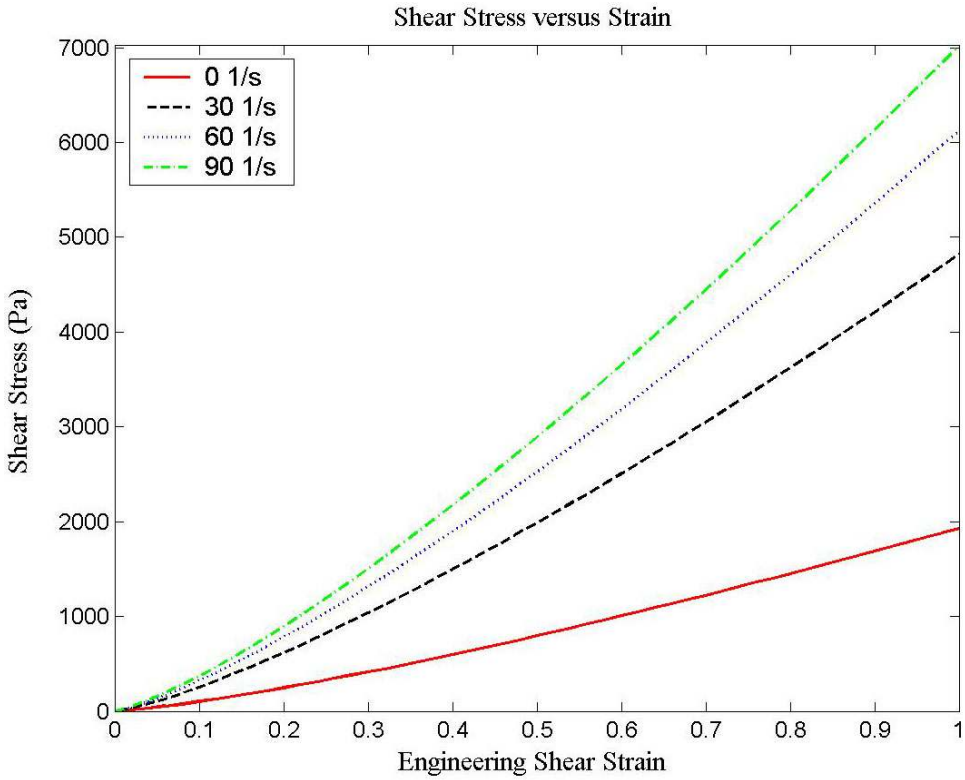

Figure 7 – Strain rate sensitivity of brain tissue in shear (Redrawn from Donnelly and Medige, 1997).

Stress relaxation

Galford and McElhaney (1970) performed relaxation tests on human and monkey brain tissue in order to study the viscoelastic properties (Fig. 8). Those experiments indicated that monkey brain is slightly stiffer than human brain. This is thought to be due to the time after death effect. The monkey brain specimens were tested within 1 hr after sacrifice while the human material was tested approximately 6-12 hr after death.

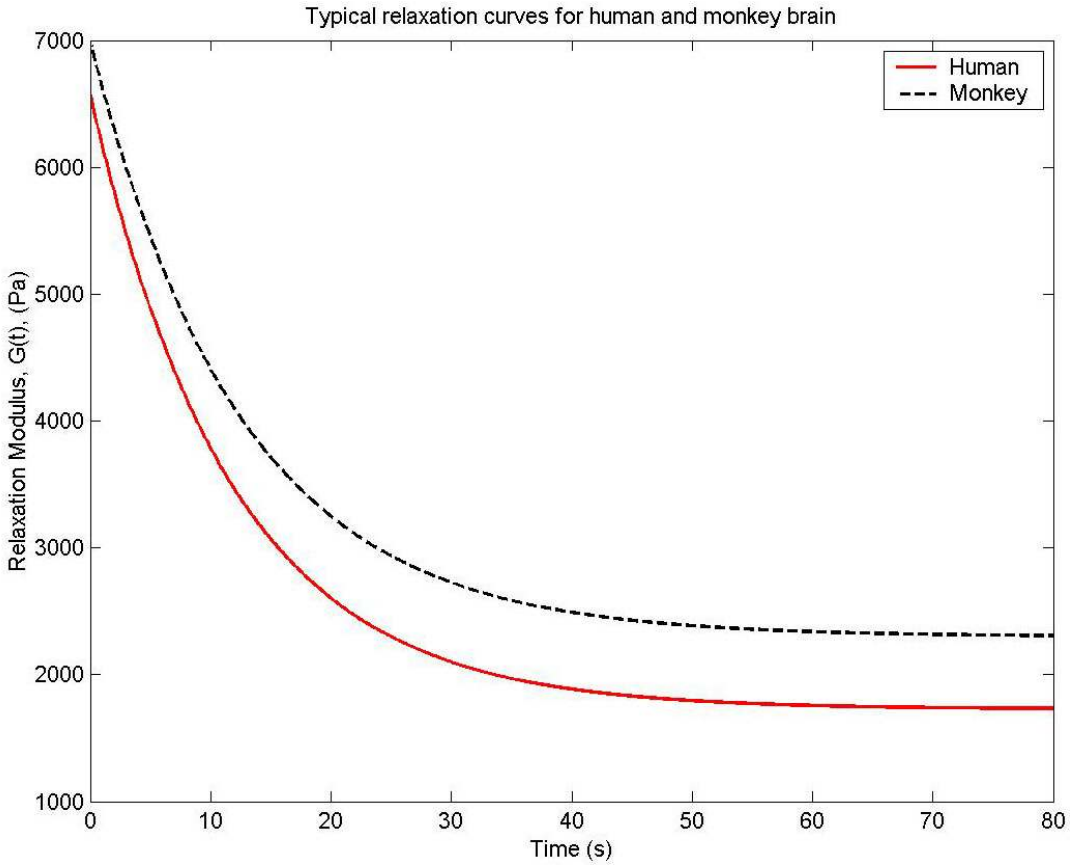

Figure 8 – Stress relaxation of brain tissue in compression (Redrawn from Galford and McElhaney, 1970).

A summary of the properties of brain tissue determined in different studies can be seen in Table 2 below.

Table 2 – Summary of properties of brain tissue

Authors	*f (Hz)*	*G' (kPa)*	*G'' (kPa)*	*Method*
Fallenstein *et al*. (1969)	9.0-10.0	0.6-11.0	0.35-6.0	Shear
Shuck, Advani (1972)	5.0-350.0	7.6-33.9	2.8-81.6	Torsion
Fitzgerald, Ferry (1953)	10.0	1.17	0.6	Shear
McElhaney *et al.* (1973)	9.0-10.0	0.43-0.95	0.35-0.6	Shear
Galford, McElhaney (1970)	34.0	22.3	8.7	Compression
Donnelly, Medige (1997)	0.0-90.0 1/s	1.8		Shear

Bridging veins

Due to the fact that acute subdural hematoma together with diffuse axonal injury account for more head injury deaths than all other lesions combined (Gennarelli, 1981), the properties of the bridging veins have been studied by several researchers. Lee and Haut (1989) studied the effects of strain rate on tensile failure properties of human bridging veins. They concluded that the failure properties were independent of the strain rate ($\dot{\varepsilon}$=0.1-250 s^{-1}), and determined the ultimate strain to be about ε_f=0.5 and the ultimate stress to be about σ_f=3.3 *MPa*. A typical load-strain curve can be seen in Fig. 9. Earlier research done by Löwenhielm (1974a) showed that the failure strain was markedly reduced as the rate was increased. He found the failure strain to vary from about 0.8 for a strain rate of $\dot{\varepsilon}$=1 s^{-1} to about 0.2 for $\dot{\varepsilon}$=1000 s^{-1}.

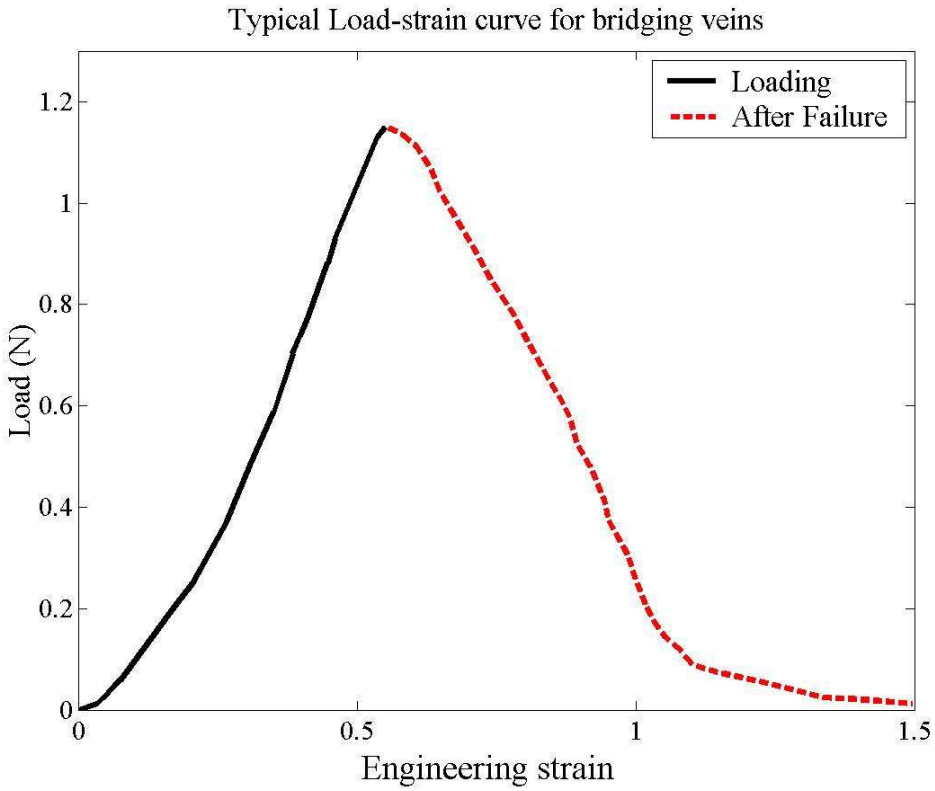

Figure 9 – Characteristic load-strain curve for bridging veins (Redrawn from Lee and Haut, 1989).

1.5 Brain injury mechanisms

Clinically brain injuries can be classified in two broad categories: focal injuries and diffuse injuries. The focal brain injury is a lesion causing local damage which can be seen by the naked eye. The diffuse brain injury is associated with global disruption of brain tissue usually and is invisible. The focal injuries consist of epidural hematomas (EDH), subdural hematomas (SDH), intracerebral hematomas (ICH), and contusions (coup and contrecoup). The diffuse injuries consist of brain swelling, concussion, and diffuse axonal injury (DAI) (Melvin *et al.*, 1993).

Focal injuries

Subdural hematoma (SDH)

The most common mechanism of subdural hematoma is tearing of veins that bridge the subdural space as they go from the brain surface to the various dural sinuses, see Fig. 10. The mortality rate in most studies is greater than 30 %.

Epidural hematoma (EDH)

Epidural hematoma is a relatively infrequently occurring sequel to head trauma (0.2-6 %, Cooper, 1982). It occurs as a result of trauma to the skull and the underlaying meningeal vessels and is not due to brain injury.

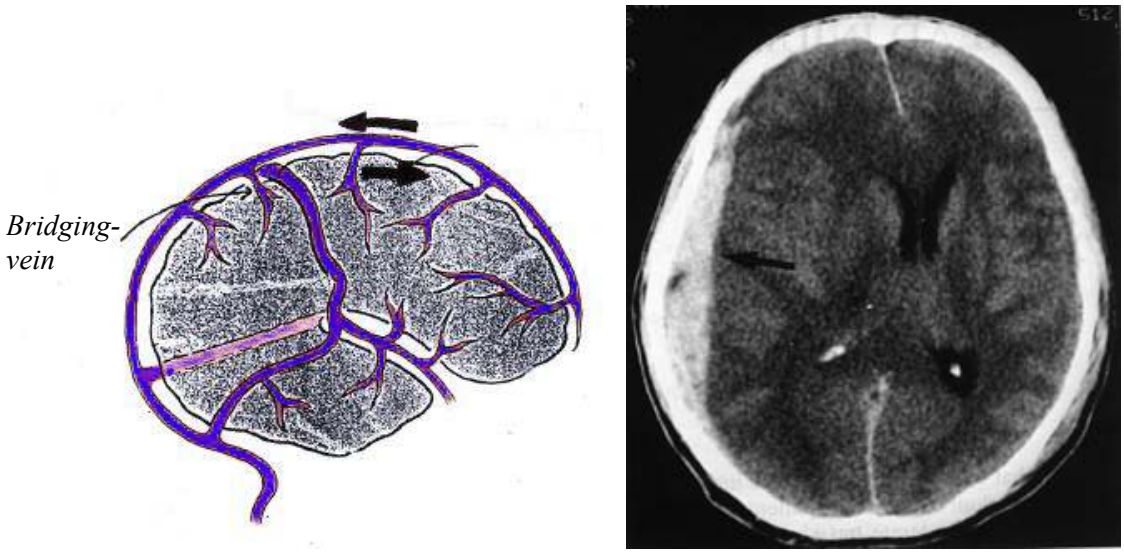

Figure 10 – Biomechanics of Subdural Hematoma.

Contusions

Cerebral contusion is the most frequently found lesion following head injury. It consists of heterogeneous areas of necrosis, pulping, infarction, hemorrhage and edema. Contusions generally occurs at the site of impact (coup contusions) and at remote sites from the impact (contrecoup contusions), see Fig. 11. The contrecoup lesions are more significant than the coup lesions.

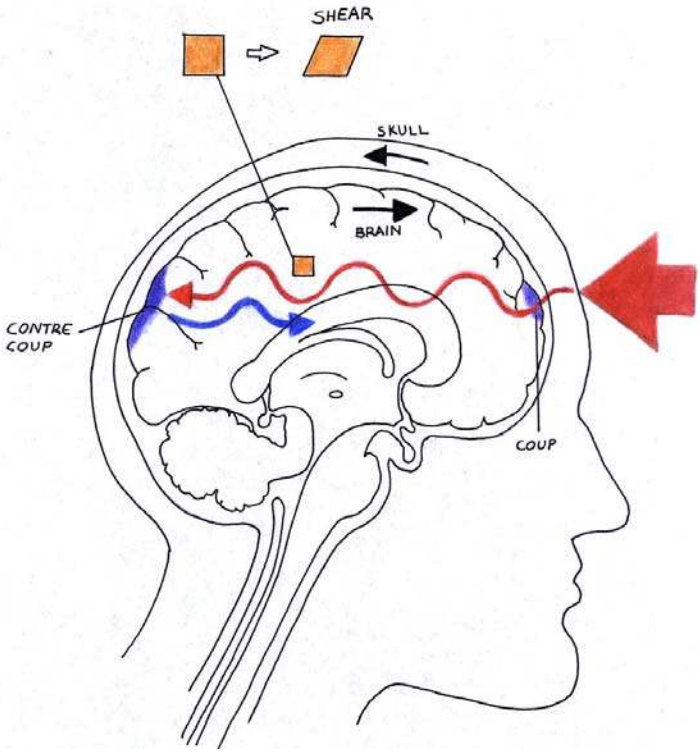

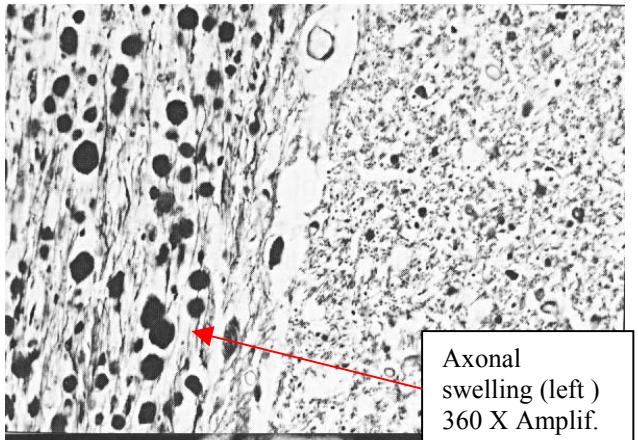

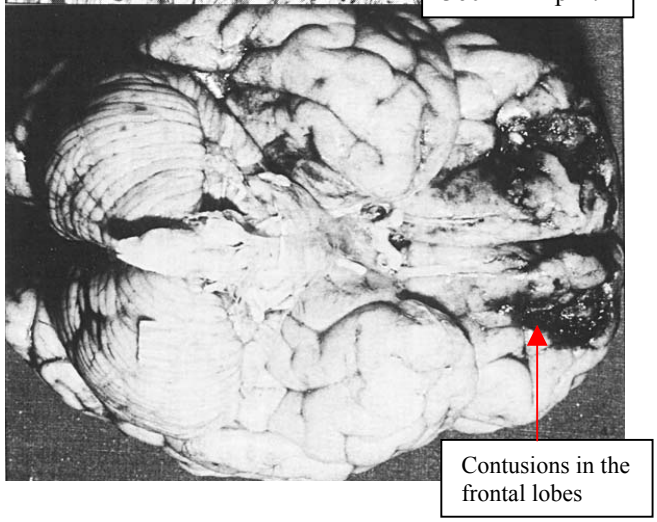

Figure 11 – Biomechanics of Contusions & DAI.

Intracerebral hematomas (ICH)
Intracerebral hematomas are well defined homogeneous collections of blood within the cerebral parenchyma. They are most commonly caused by sudden acceleration/deceleration of the head. Other causes are penetrating wounds and blows to the head.

Diffuse Injuries
Concussion
The classical cerebral concussion is the most common head injury diagnosis, and involves immediate loss of consciousness following injury. In general, 95 % of the patients have good recovery at the end of 1 month. More than 99% of the patients have left the hospital within 14 days (Kleiven *et al.*, 2002).

Diffuse axonal injury (DAI)
Diffuse axonal injury is associated with mechanical disruption of many axons in the cerebral hemispheres and subcortical white matter (Fig. 11). Microscopic examination of the brain discloses axonal tearing throughout the white matter of both cerebral hemispheres. It also involves degeneration of long white matter tracts extending into the brain stem. High-resolution CT scans may show small hemorrhages and axonal swelling (Fig. 11). DAI involves immediate loss of consciousness lasting for days to weeks. Severe memory and motor deficits, is present, and posttraumatic amnesia may last for weeks. At the end of 1 month, 55 % of the patients are likely to have died (Gennarelli *et al.*,1982).

Brain swelling
Brain swelling (=edema), or an increase in intravascular blood within the brain adds to the effects of the primary injury by increased intracranial pressure.

1.6 Head Injury Criteria

Abbreviated Injury Scale (AIS)
The Abbreviated Injury Scale is an empirically-based categorical scale that assigns an injury severity rating on the basis of the observed injuries sustained by the experimental subject following the test.

The AIS is a categorical index ranging from 0 to 6, where
0 = No injury
1 = Minor injury
2 = Moderate injury
3/4 = Serious/Severe injury
5/6 = Critical/Fatal injury

Examples of the most common AIS 1-3 injuries are neck or back pain and minor concussion. Examples of common AIS 4-6 injuries include concussion (unconscious 12 hours), fractured vertebrae, and cerebellur lesion.

Head Injury Criteria (HIC)

The most common criterion used to predict head injuries is *the Head Injury Criterion (HIC)* (1972, National Highway Traffic Safety Adm.). Researchers used an indirect approach to study human concussion by impacting embalmed cadaver heads, and look for skull fractures. The rationale for using this indirect approach was based on the clinical observation that concussion is present in 80 % of patients with simple linear skull fractures. It is based on the resultant translational acceleration of the head. The HIC should not exceed 1000 if the integration limits are separated no more than 36 ms. The acceleration, a, in this formula is given in g.

$$HIC = \mathbf{max}\left[\frac{1}{(t_2 - t_1)}\int_{t_1}^{t_2} a(t)dt\right]^{2.5}(t_2 - t_1) \qquad (1.1)$$

HIC was first introduced as a curve fit to the Wayne State Tolerance Curve (WSTC). The WSTC (Fig. 12) was first presented by Lissner (1960), and was generated by dropping embalmed cadavers onto unyielding, flat surfases, striking the subject on the forehead. Gadd (1966) developed the Severity Index (SI) to fit the WSTC (Fig. 12), with a value greater than 1000 considered to be dangerous to life. It was not only based on the WSTC, but also upon additional long pulse duration data by means of the Eiband (1959) tolerance data and other primate sled test data. The SI provided a good fit for both the short duration skull fracture data and the longer duration Eiband data out to 50 ms duration.

The WSTC provided a relationship between peak acceleration, pulse duration, and concussion onset. In the final form, the WSTC was developed by combining results from a wide variety of pulse shapes, cadavers, animals, human volunteers, clinical research, and injury mechanisms.

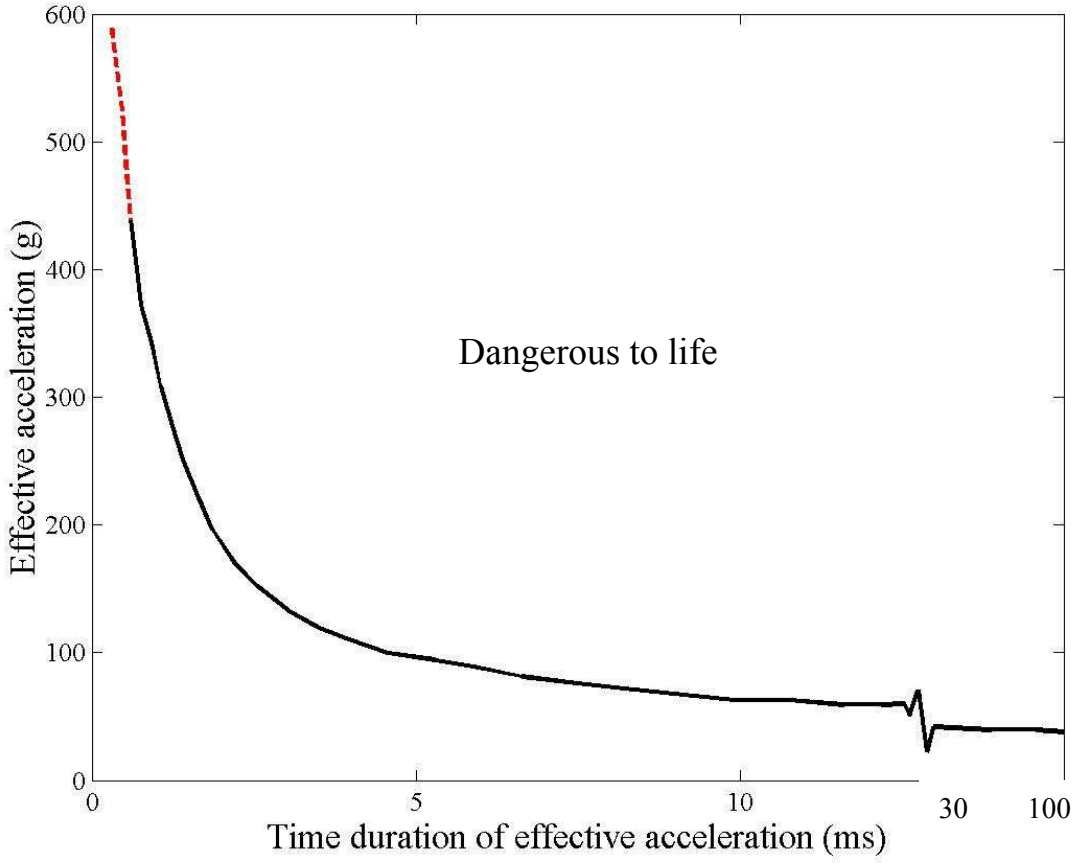

Figure 12 – The Wayne State Tolerance Curve (Redrawn from Versace, 1971).

Proposed Limits for HIC

Limits for various sizes of the human head were proposed for HIC_{36} by Kleinberger *et al.* (1998) and for HIC_{15} by Eppinger *et al.* (2000) using the HIC scale factor $\lambda_{HIC}=(\lambda_E)^2/(\lambda_L)^{1.5}$ derived by Melvin (1995). The modulus of elasticity scale factor is $\lambda_E=E_1/E_2$, and the length scale factor is $\lambda_L=L_1/L_2$, and the subscripts 1 and 2 refer to the subjects to be scaled to and from. One might discuss the validity of these limits for most brain injury mechanisms since the elasticity scale factor only takes into account the skull material properties.

Table 3 – Proposed limits for HIC (From Kleinberger *et al.*, 1998, and Eppinger *et al.*, 2000).

Dummy Type	*Mid-sized Male*	*Small female*	*6 year old child*	*3 year old child*	*12 month old child*
HIC_{36}	1000	1000	1000	900	660
HIC_{15}	700	700	700	570	390

A_{3ms} – Maximal Acceleration for >3ms

The resultant acceleration shall not exceed 80g for more than 3 milliseconds (ms). From additional animal studies and analytical calculations to the strain in the skull (DOT contract FH-11-7288 presented in Stalnaker *et al.*, 1971), it was concluded that the asymptotic value of 42g for the longer durations in the WSTC was probably too low (Fig. 12). Therefore a value of 60-80g was estimated as a limit of concentrated loads for longer durations than 3ms (Versace, 1971).

A_{max} – Peak Acceleration

A separate tolerance for peak acceleration to avoid skull fracture is set. Recent studies by Mertz *et al.* (1997) estimates a 5% risk of skull fractures for a peak acceleration of about 180g, and a 40% risk of fractures for a peak acceleration of 250g.

Head Impact Power (HIP)

Recently a new global head kinematic-based injury potential measure, called the Head Impact Power (HIP) was presented (Newman *et al.*, 2000). In that study, it was proposed that coefficients for the different directions could be chosen to normalize the HIP with respect to some selected failure levels for a specific direction. However, values of the coefficients were not presented and information regarding directional sensitivity was lacking.

$$HIP = ma_x \int a_x dt + ma_y \int a_y dt + ma_z \int a_z dt + I_{xx}\alpha_x \int \alpha_x dt + I_{yy}\alpha_y \int \alpha_y dt + I_{zz}\alpha_z \int \alpha_z dt \qquad (1.2)$$

The x-axis was defined along the Posterior-Anterior (PA) direction, the y-axis along the lateral-direction, and the z-axis in the Inferior-Superior (IS) direction.Head injury is assumed to correlate with the maximum value of HIP achieved by equation 2 during an impact, named HIP_{max}.

Generalized Acceleration Model for Brain Injury Threshold (GAMBIT)

This was an early effort to combine thresholds for translational and rotational kinematics (Newman, 1986). Although a step in the right direction, it had some limitations in the lack of data used to derive the thresholds, lack of impulse duration dependency, as well as in lack of accounting for directional sensitivity. Maybe due to these problems, as well as conservatism among car manufactures and legislation makers, it never became widely accepted by the general public.

The GAMBIT requires to establish the maximum value, G, of the function *G(t),* i.e. *G=max[G(t)]*. *G*=1 is normally set to correspond to a 50% probability of AIS>3. Some versions of *G(t)* have been presented (Newman, 1986, 2000), but the most general one is:

$$G(t) = [(\frac{a(t)}{a_c})^n + (\frac{\alpha(t)}{\alpha_c})^m]^{1/s} \qquad (1.3)$$

where a(t) and α(t) are the instantaneous values of the translational and rotational acceleration, respectively, and n, m, and s are empirical constants selected to fit available data. The a_c and α_c are the acceleration thresholds for a pure translational, and a pure rotational impulse, respectively. Proposed values for the constants are: n=m=s=1, a_c=250g and α_c=10000r/s^2 (Newman, 1986), and n=m=s=2, a_c=250g and α_c=25000r/s^2 (Newman *et al.*, 2000). Since no dependency of the impulse duration is included, the GAMBIT can be seen as a peak-acceleration criterion for a combined rotational and translational impulse.

Skull and Brain Compliance Models

Stalnaker and McElhaney (1970) and Stalnaker *et al.* (1971) used forced-vibration response data of human and animal heads to fit parameters of mechanical impedance models. The resonance data were used to develop lumped mass models called the Mean Strain Criterion (MSC) and the New Mean Strain Criterion (NMSC), Stalnaker *et al.* (1987). The MSC consisted of a damper and a spring coupled in parallell between lumped masses of frontal parts of the skull and the rest of the skull and the brain, while the NMSC consisted of an additional damper. The maximum strain observed between the lumped masses, due to input velocity and displacement was interpreted as a risk of injury.

Viano (1988) added a viscous damper and bilinear spring to produce the Brain Compliance Model (BCM). The parameters in the BCM had lower values, which were argued to be more related to the brain response. Also, the addition of an elastic element (bilinear spring) allowed restoration of the brain in the BCM, while the MSC and NMSC did not.

The brain compliance model, translates the effect of rapid skull motion as tissue-level deformations of the brain. The brain compliance approach interprets brain deformation by the viscous response (VC) or the product of strain and strain rate at the tissue- level. The viscous response is the product of tissue deformation, V, and compression, C (Viano and Lau, 1988). VC is proportional to the energy absorbed by brain tissue during rapid deformation. Locally, VC is the product of strain and strain rate, $\varepsilon \cdot d\varepsilon / dt$. Viano *et al*., (1996) gives proposed injury tolerances of VC=0.7 m/s, and $\varepsilon \cdot d\varepsilon / dt$ =45s^{-1}.

Angular acceleration thresholds

Proposed Threshold for DAI

Margulies and Thibault (1992) presented a criterion for DAI. It is developed using experiments on primates in combination with gel physical models and analytical scaling procedures. Judging from Fig. 13, rotational accelerations exceeding 10 krad/s^2 combined with an angular velocity of 100 rad/s or higher gives a risk of DAI in the adult. These curves show that for small changes in angular velocities the injury is less dependent on the peak angular acceleration, while for high values of peak change in angular velocity, the injury is sensitive to the peak angular acceleration. This is in agreement with the hypothesis of Holbourn (1943). He stated that the shear strain, and thus injury, for long duration impulses (large peak change in rotational velocity) is proportional

to the acceleration, while the injury is proportional to the change of velocity of the head for short duration impacts.

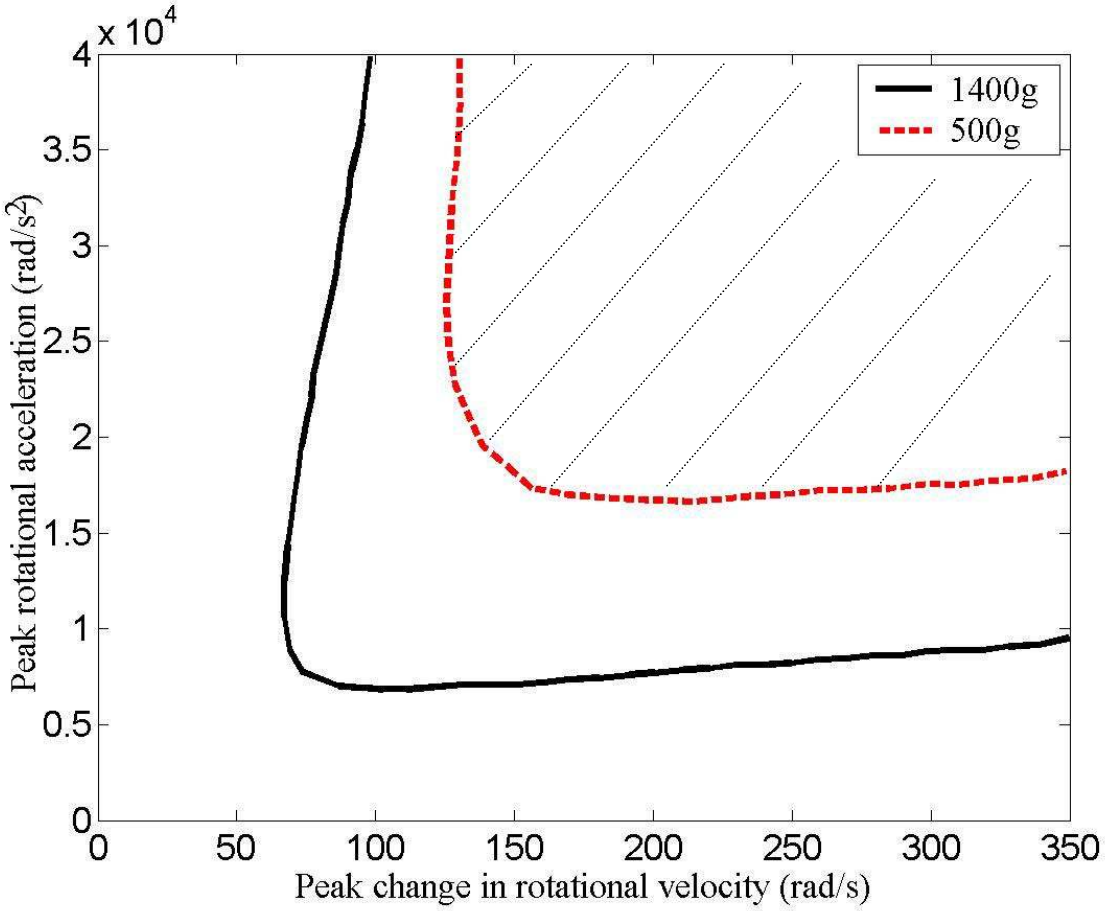

Figure 13 – Modified from Margulies and Thibault (1992). The full line represents the limit for an average adult (brain mass 1400g).

Proposed Threshold for SDH

In a primate study (Gennarelli and Thibault, 1982), it was proposed that an angular acceleration exceeding 175 krad/s^2 combined with an impuls time exceeding 5ms, would produce SDH in the rhesus monkey. Interestingly, the threshold for SDH in the rhesus monkey seemed to increase with the duration of the impulse, which is the opposite of other head injuries such as skull fracture and concussion (confer the WSTC in Fig. 12). This phenomenon can also be seen in experiments on human cadavers reported by Löwenhielm (1974b) and experiments on squirrel monkeys reported by Unterharnscheidt and Higgins (1969). The results from the experiments by Gennarelli and Thibault (1982) are seen in Fig. 14.

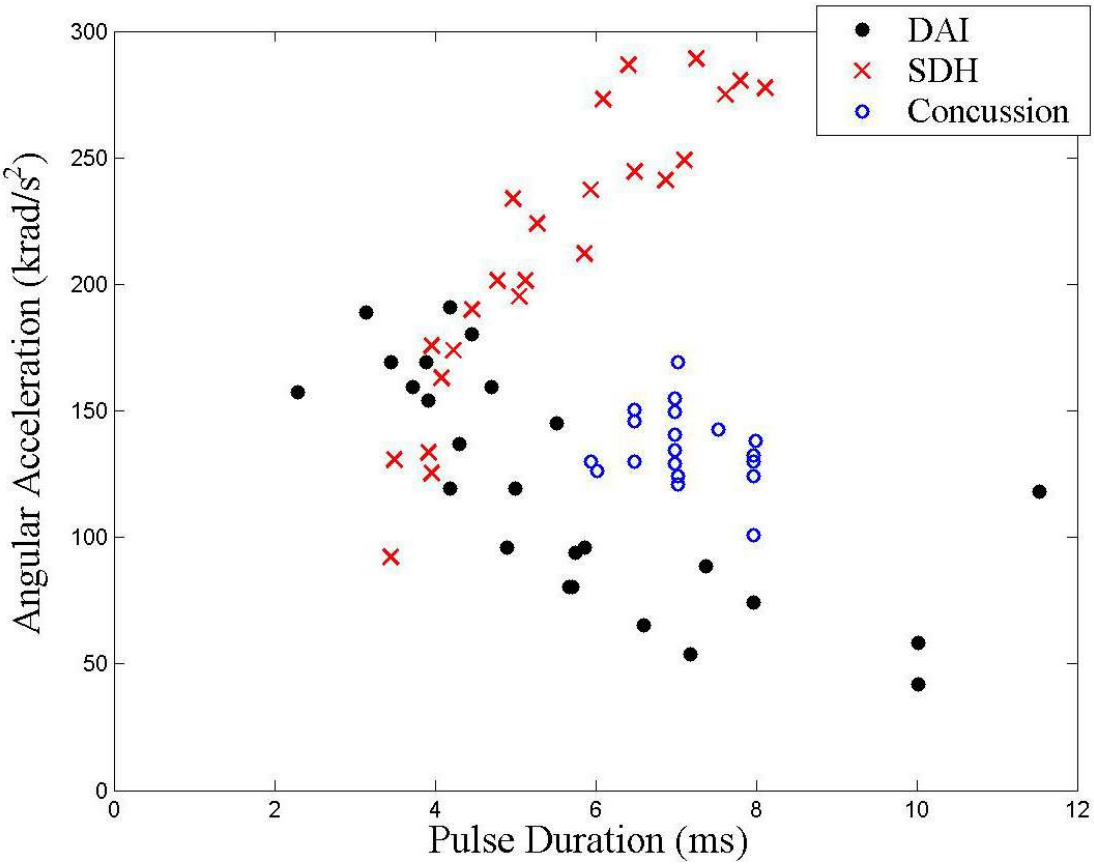

Figur 14 – Redrawn from results presented in Gennarelli and Thibault (1982).

Löwenhielm (1974b) stated that bridging vein disruption due to rotational movement of the head is obtained when the angular acceleration exceeds 4.5 krad/s^2 and/or the change in angular velocity exceeds 50 rad/s using collision tests with cadavers. The estimation of the rotational accelerations/velocities were based on differentiation of smoothed cubic spline interpolations (of head rotations) of high speed videos (500 frames/s) of the plane motion of the head in the sagittal plane. Thus leaving out any synergic effects of other rotations/translations. On the other hand, the motions were not pure rotational, and either none or several bridging veins were ruptured indicating that a real threshold never was found. Also, in these experiments which were previously presented by Voigt and Lange (1971), there were a high level of violence other than the rotational. The non-belted cadavers were seated on a sled and accelerated to velocities of between 43 to 60 km/h before braked into standstill and impacting towards the instrument panels. In some of these experiments the translational acceleration on the top of the head was recorded. In the more severe cases, translational accelerations varying between +/- 200g was recorded, adding to the rotational violence.

Proposed Thresholds for Concussion

Ommaya *et al.* (1967), and Ommaya and Hirsch (1971) proposed limits for angular acceleration (α). A more than 99% probability of concussion was estimated for α>7500 r/s^2, when the impulse duration exceeds 6.5ms (Ommaya *et al.*, 1967). Also, a limit of α>1800 r/s^2 to produce concussions due to head rotation induced by whiplash was proposed (Ommaya and Hirsch 1971).

Since all angular thresholds are based on non-centroidal rotation in primate experiments followed by analytical scaling techniques, the applicability of thresholds for humans might be discussed. Also, later studies on volunteer boxers (A.P.R., 1988 and Pincemaille *et al.*, 1989) suggests that

the human tolerance is largely underestimated using primate experiments and simplistic scaling rules.

1.7 Review of Finite Element Models of the Human Head

In order to define the state of the art and to get a brief overview of research findings within the area of finite element modeling of the human head, a literature survey was conducted.

Although the FE modeling of the human head has been advancing over the past decades, it is still far from being able to explain brain injury mechanisms and predict impact injuries. From this review, it can be pointed out that material modeling, skull-brain interface conditions, pressure release through foramen magnum, the effects of ventricles and the subarachnoid space, the effects of a three layered skull including sutures and authentic geometry etc. needs further investigation. However, using proper material characterization, correct boundary conditions and detailed geometric representation, a finite element model of the human head can provide us a powerful tool.

The first mathematical model of the human head is thought to be the model of a spherical liquid mass by Anzelius (1943). He analyzed the pressure response due to an abrupt change in velocity, and found that positive pressure occurred close to the impact, while a negative pressure appeared at the contrecoup location. It was also calculated that a node of zero pressure was produced at the center of the sphere. Analytical models are, however, limited to problems with relatively regular geometry, simple boundary conditions and homogeneous material properties, because of the mathematical difficulties in formulation and solution. Numerical approaches, on the other hand, approximate the analytical solution with a numerical procedure. Finite element modeling of the human head has gradually progressed. The first three dimensional models had simplified and regular geometry: a spherical, spheroidal or ellipsoidal shell for the skull (Chan, 1974; Kenner and Goldsmith, 1972; Khalil and Hubbard, 1977). Other early works are based on the actual geometry of the human head (Hardy and Marcal, 1973; Hosey and Liu, 1981; Nickell and Marcal, 1974; Shugar, 1975, Ward, 1982). These models, apart from Hosey and Liu (1981), considered the anatomical and material features of only one of the two major structures: the skull or the brain. In all these models, linearly elastic or linearly viscoelastic properties were assigned to the skull and brain, or the brain was modeled as an inviscid fluid inside an encased elastic layer. Khalil and Viano, (1982) and Voo *et al.*, (1996) have reviewed these older models. Only reports which are published after 1989 are therefore included in this review. The FE models were compared by general aspects as the geometry modeled, constitutive modeling, interface conditions and significant findings.

Geometry & components modelled
Only 3D FE models of the human head are relevant for most impact and inertial load analysis. Due to the low shear resistance and large bulk modulus material exchange between regions is likely to occur (CSF, foramen magnum etc.), when subjected to large deformations. This can only be described from a 3-D point of view. However, 2D models are useful for parametric studies of controlled planar motions. Also, 2D models simplifies the inclusion of geometrical details compared to a corresponding 3D model. Different internal components should be modeled separately. Zhou *et al.*, (1995) showed that differentiation between gray and white matter and inclusion of the ventricles are necessary to match regions of high shear stress to locations of DAI. On the other hand, the ventricles were modeled with linear elastic solid elements (not fluid elements) and the Young's modulus of the white matter was assumed to be 60 % higher than that

of the gray matter. A summary of the significant findings for 2D models, and 3D models can be seen in tables 4 and 5, respectively.

Table 4 – Summary of two-dimensional finite element models of human and animal heads.

Authors	Geometry	Const. Mod.	Validation	Findings
Ueno *et al,*. 1989, 1995	Sagittal Human	Rigid, linearly elasic	Pressure	Transl. Acc. Rel. to pressure Rot. Acc. Rel. to shear. Combined acc. gives largest values
Cheng *et al* ., 1990	Coronal Half Cyl.	Rigid, linearly viscoelasic	Against cyl. gel model	Skull/brain interface, geometry important for brain response
Ruan *et al* . 1991	Coronal Human	Inviscid fluid, linear elastic	Not performed	Membranes needs to be included for "correct" dynamic response
Willinger *et al.* 1992	Sagittal Human	Linear elastic	Not performed	Occ. Impacts lead to frontal inj. Res. Freq. dep. on subarachn. CSF
Chu *et al* . 1994	Parasagittal Human	Linear elastic	Pressure	Shear strain account better for contusions than pressure
Kuijpers *et al* . 1995	Parasagittal Human	Linear elastic viscoelastic	Pressure	Pressures more sensitive to skull-brain interface than foramen magnum
Zhou *et al.* , 1994 Al-Bsharat *et al.* , 1997	Coronal Porcine	Linear elastic viscoelastic	Not performed	Maximum shear strain matched areas of damage in animal experiments
Miller *et al* . 1998, 1999	Axial Mini. Pig	Rigid, lin. el. hyperviscoel.	Not performed	Frictional interface predicted DAI injury pattern best
Prange *et al.* 1999	Coronal Human	Rigid, hyperviscoel.	Not performed	Larger strains in adult model than pediatric

Bandak *et al.* (1995) and Krabbel *et al.* (1995) developed procedures for generating a detailed FE model of the human skull from CT scan images, but such procedures requires CT scans of the geometry you want to generate/simulate. This might be a great limitation if an average model is wanted, or if variational studies are of interest. However, neither of these models explicitly take into account the different parts of the CNS tissue. Procedures that automatically generate a FE model of complex geometries have also shown to have problems in creating a well conditioned element mesh. Kumaresan *et al.* (1995) used the upper limits of the landmark coordinates of the external geometry of a dummy head (Hubbard and McLeod, 1974), and divided the the head in 33 layers in the horizontal plane. The coordinates of the curves connecting the exterior landmarks were calculated on an incremental basis (5 mm). The coordinate values of all the points on the curvature in the different layers of the head were given as input to the preprocessor of a FE package to generate the model. These points were joined together by parabolic cubic lines to form the outer curvature of the head. This approach gives a more flexible model. However, more details and a general model can be generated by incorporating interior landmarks, variational parameters and all the geometric features of the brain.

Table 5 – Summary of three-dimensional finite element models of human and animal heads.

Authors	Geometry	Const. Mod.	Validation	Findings
DiMasi *et al* ., 1991, 1995, Bandak *et al.,* 1994	3D human	Rigid skull, linearly elasic membranes, viscoelastic brain	Not performed	Proposed a cumulative measure (CSDM) Translational acc. small influence on CSDM Sagittal rot. gave higher CSDM than coronal
Ruan *et al* ., 1994, 1997, Ruan, Prasad, 1995, 2001	3D 50th perc. male	Linearly elastic, viscoelasic	Pressure	Stiffness of skull affects intracranial pressure Higher Contrecoup pressure from occ. impact Decreased skull def. with increased thickness
Bandak *et al.,* 1995	3D detailed	Linearly elastic	Not performed	Present a procedure for generating a 3D FE model of the human skull from CT images
Kumaresan *et al.,* 1995	3D detailed	Not assigned	Not performed	Describe a procedure for generating a 3D FE model of the human head
Willinger *et al.,* 1995, 1999 Turquier *et al.,* 1996	3D human	Linearly elastic, viscoelasic	Pressure	Proposed physical head model that replicate resonance frequencies calc. by FEM
Ueno *et al.,* 1995	3D ferret	Rigid skull, linearly elasic brain,	Kinematics of impactor	Pattern of shear similar to pattern of contusion seen in the experiments
Zhou *et al.* , 1995, 1996 Al-Bsharat *et al.* , 1999	3D 50th perc. male	Linearly elastic viscoelastic	Pressure Rel. motion magnitude	Differentiation of CNS and ventricles affects stress distribution. Sagittal rot. Cause higher strain in bridging veins than coronal rot. Higher stress in corpus c. for sag. Rot. than cor.
Claessens *et al* . 1997	3D human	Linearly elastic	Pressure	Skull-brain interface has greater influence on intracr. pressure than an exact internal geom.
Huang *et al.* 1999, 2000 Model: Shugar (1977)	3D human	Linearly elastic	Pressure	Contribution of rotational acc. to tearing of bridging veins greater than that of trans. acc. Shear strain account better for contusions
Zhang *et al* ., 2001a Zhang *et al* ., 2001b	3D human	Linearly elastic viscoelastic	Pressure	Higher stress and pressure for a lateral imp. compared to a frontal. Capability of simulating fractures of facial bones

Material modeling & Interface conditions

The FE modeling made in the reviewed publications have all assumed isotropic, linear elastic or linear viscoelastic and homogeneous material properties within each modelled component. Isotropic material properties is an approximation which can be justified for most of the components but orthotropic properties can be used for fibrous materials without increased CPU cost. Nonlinear material properties should also be preferred for areas which undergo large deformation. For the CSF, fluid elements could be used (as proposed by Zhou *et al.*, 1995 and Bandak and Eppinger, 1994) in order to investigate the effect of ventricles, subarachnoid space, skull/brain interface etc. in a proper way. The properties for brain tissue, and interface conditions used in 2D, and 3D models are summarized in tables 6 and 7, respectively.

The skull-brain interface of the Human Head

Relative motion between the skull and the brain during impact, has been observed since more than fifty years ago (Pudenz and Shelden, 1946, Gurdjian *et al.,* 1968). Recognizing this gives a special interest in how to model this feature in an FE model of the human head. The approach of modeling the CSF using linear elastic solid elements with low shear modulus (Ruan *et al.*, 1991, 1993, 1995, 1997, 2001; Willinger *et al.*, 1992, 1995; Turquier *et al.*, 1996; Zhou *et al.*, 1995, Zhang *et al.*, 2001) has shown to induce shear stress/strain in the interface (even with a low shear modulus), and is also likely to cause computational instability because of large element distortions. Another way of modeling the skull-brain interface includes contact algorithms between the brain and the dura mater. The contact definition has been modeled in different ways ranging from completely fixed to frictionless sliding. Several parametric studies have been performed, where the effect of different interface conditions between skull and brain has been studied (Bandak and Eppinger, 1994; Miller *et al.*, 1998; Cheng *et al.*, 1990; DiMasi *et al.*, 1991;

Kuijpers *et al.*, 1995; and Claessens, 1997). All of them conclude that the impact response of the human head is sensitive to the modeling of this interface condition.

Table 6 – Summary of properties, and interface conditions used in two-dimensional finite element models of human and animal heads.

Authors	Brain tissue prop.	Skull-brain interface	Foramen magnum
Ueno *et al.*, 1989, 1995	G=80 kPa, ν=0.49	Tied nodes	Free nodes at Foramen
Cheng *et al*., 1990	G_∞=16.2 kPa, G_0=49.0 kPa	Both tied and sliding were studied	Not modeled
Ruan *et al*., 1991	β=145.1/s E=60.7 kPa ν=0.48	CSF modeled as a solid	Not modeled
Willinger *et al.*, 1992	E=675 kPa ν=0.48	CSF modeled as a solid	Not modeled
Chu *et al*., 1994	E=250 kPa ν=0.49	Tied nodes	Free nodes at Foramen
Kuijpers *et al*. 1995	G_∞=169 kPa, G_0=338 kPa β=50-10000 1/s, ν=0.48	Both tied and sliding were studied	Both free nodes and tied nodes were studied
Zhou *et al.*, 1994 Al-Bsharat *et al.*, 1997	G=168-268 kPa, G_∞=6-8 kPa, G_0=33-43 kPa	Tied nodes Sliding	Not modeled Not modeled
Miller *et al*., 1998, 1999	β=700 1/s, ν=0.4996 Hyperviscoelastic accord. to Mendis *et al.* (1995)	Both CSF modeled as a solid and sliding cont. were studied	Not modeled
Prange *et al.*, 1999	Hyperviscoelastic	Sliding with friction	Not modeled

The study performed by Kuijpers *et al.* (1995) used a 2D finite element model of a parasagittal cross section of the human head. The skull-brain interface was modeled in two ways; 1. As completely coupled and 2. With a sliding contact condition allowing for separation. Further on, the foramen magnum was modeled in three ways; 1. Rigidly coupled, 2. With a sliding contact condition allowing for separation, and 3. With a force free foramen magnum. Simulations of impacts to the frontal bone of human cadavers (Nahum *et al.*, 1977) were performed utilizing combinations of the different interface conditions. Comparison with the experiments showed good agreement for the coup pressure when using the sliding contact conditions, while the models with coupled interfaces showed poor agreement with the experiments. None of the models were able to simulate the magnitude and characteristics of the contrecoup pressure obtained in the experiments. This could be the lack of ability to carry load in tension by the contact algorithm. The authors concluded that both the coup and contrecoup pressures were found to be more sensitive to the type of skull-brain interface condition in comparison to the presence or absence of a force-free foramen magnum

Table 7 – Summary of properties, and interface conditions used in three-dimensional finite element models of human and animal heads.

Authors	Brain tissue prop.	Skull-brain interface	Foramen magnum
DiMasi *et al*., 1991, 1995 Bandak *et al.,* 1994		Ranging from sliding to fixed	Not modeled
Ruan *et al*., 1994, 1997, Ruan, Prasad, 1995, 2001	G_∞=17.4 kPa, G_0=34.8 kPa β=100 1/s, K=2.19 Gpa	CSF modeled as a solid	Upper part of brain stem is modeled
Bandak *et al.,* 1995	E=168 kPa, G=528 kPa E=68 MPa, ν=0.45	Common nodes	Open boundary
Kumaresan *et al.,* 1995	None assigned	CSF modeled as a solid	No information
Willinger *et al.,* 1995, 1999 Turquier *et al.,* 1996	E=675 kPa ν=0.48 G_∞=168 kPa, G_0=528	CSF modeled as a solid	Not modeled
Ueno *et al.,* 1995	E=80 kPa ν=0.49	Interface gap.	Free nodes at Foramen
Zhou *et al.*, 1995, 1996 Al-Bsharat et al., 1999	G=168-268 kPa	Ranging from tied nodes to sliding without separation	Upper part of brain stem is modeled
Claessens *et al*. 1997	G_∞=6-8 kPa, G_0=33-43 kPa E=1.0 MPa ν=0.48 β=700 1/s, ν=0.4996	Ranging from sliding to fixed	Upper part of brain stem is modeled
Huang *et al.* 1999, 2000 Model from Shugar (1977)	E=0.25 MPa ν=0.49	Common nodes	Not modeled
Zhang *et al*., 2001a Zhang *et al*., 2001b	 G_∞=6-8 kPa, G_0=33-43 kPa β=700 1/s, K=2.19 GPa G_∞=2-2.5 kPa, G_0=10-12.5kPa β=80 1/s	Tied interface Sliding without separation	Upper part of brain stem is modeled

Claessens *et al.* (1997) did a study similar to the one performed by Kuijpers *et al.* (1995) but used instead a 3D FE model of the human head. Two different approaches were used for the skull brain interface: 1. A coupled interface, allowing no relative motion between the skull and the brain, and 2. A sliding contact condition allowing for separation, and the models were subjected to a frontal impact as in the experiments of Nahum *et al.* (1977). The results obtained with this 3D FE model contrasted with those obtained by Kuijpers *et al.* (1995). The no-slip model showed good agreement with the experiments for the coup pressures, while the sliding interface model did not. On the other hand, these two studies agreed when it came to the contrecoup pressure, which not even the 3D study was able to mimic.

A recent study by Miller *et al.* (1998) compared the two commonly used strategies to model the skull-brain interface. A 2D cross section of a coronal plane was used to simulate rotational tests performed in an experimental model of severe diffuse axonal injury (DAI) in the miniature pig. The first approach modeled the subarachnoidal CSF using linear elastic solid elements with low shear modulus, while the second included a sliding contact algorithm between the brain and the dura mater with a coefficient of friction of 0.2. By comparing the maximal principal nominal strain, von Mises stress, and pressure, these two approaches were evaluated when it came to the ability of reproducing the injuries found in the experiments. The results showed that the second (sliding interface) approach was the more reliable in predicting location and distribution of axonal injury and cortical contusions. The study also found the effects of the coefficient of friction in the sliding interface to be small by varying this between 0.001 and 0.4.

Al-Bsharat and co-workers (1999) thereafter modified the model presented by Zhou *et al.* (1995), by introducing a sliding contact definition between the CSF and the pia matter in the subdural space of the brain. In this way, the sliding of the brain within the skull could be simulated.

Although being a major step forward, this model still utilizes linear viscoelastic properties for the CNS tissues. Instead of providing a fluid element formulation, the CSF is modeled as a solid with a low shear modulus. In this work the upper part of the spinal cord and the neck are not included, which could affect the pressure release through the foramen magnum.

To be able to model the foramen magnum interface realistically, experimental validation and usage of fluid flow models (as proposed by Bandak and Eppinger, 1994) seems to be a correct approach.

Inclusion of an Irregular Skullbase

Willinger and co-workers (1999) presented a validation of their 3D FE model against two experimental impacts. They discuss the simplification of this model toward the temporal lobes, and conclude that a new human head model with a more realistic brain geometry is needed to improve the model response. This FE model and others which are state of the art approximate the sharp ridges of the skull base with smoother transitions between the different fossae. Even the highly discretisized WSUBIM, version 2001 (Zhang *et al.*, 2001) have a slightly smoothed sphenoid ridge. This commonly used approximation is apparent when studying the model used in Huang *et al.* (1999, 2000), where neither the middle fossae nor the sphenoid ridge was included. It is also known that in the primates the ridges in the middle fossae are less pronounced. It is therefore interesting to study the effects of an irregular skull base.

A study of the intracranial responses when enduring an occipital impact simulating the relative motion magnitude experiments reported in Al-Bsharat *et al.* (1999), was therefore performed. A previous version of the model (Kleiven and von Holst, 2002), including the detailed skull base and the middle fossae (Fig. 2, chapter 1.4), and a model with a slightly smoothed sphenoid ridge was compared for the same occipital impact. In both models, a sliding only contact definition was utilized for the skull-brain interface. The brains of these two models can be seen in Fig. 15, below.

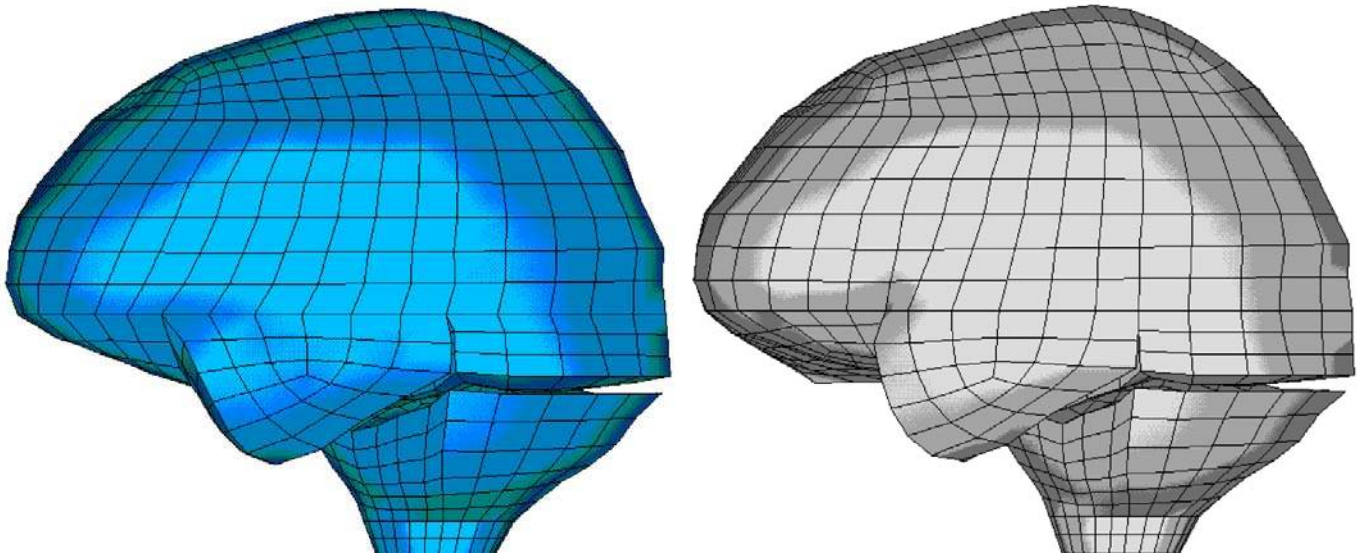

Fig. 15 – Two brains corresponding to a smoothed (left) and sharp (right) sphenoid ridge.

By taking away the sharp frontal edge of the middle fossae, this gave a 25% larger relative motion for brain tissue close to the skull base in the parieto-occipital region, while points closer to the vertex appear to be unaffected. This is a reasonable result because the differences in the models are also in the lower areas. These results are also in agreement with Ivarsson *et al.* (2001),

who used 2D physical (gel) models, and compared an irregular skull base with a version approximating the anterior and middle fossae as a flat structure.

Material Modeling
As seen in Table 6 and 7 there are great variations in the material data used. These variations must be reduced. An approach to reduce them is to detect which factors the variations depend on. This factors can be: age, sex, calcium content (for bone), location within the component (for inhomogeneous materials). Donnelly (1998) reviewed and reported the average values of the shear relaxation modulus for brain tissue. According to this study, the average value of the instantaneous shear relaxation modulus for brain tissue is around one *kPa*. Apart from the study by Prange *et al.* (1999), all FE modeling studies have included properties that are around 10-1000 times larger than the average published values. Bandak *et al.* (1995) presented a value of 68 *MPa* for the linearly elastic brain in a study of a procedure for generating a 3D FE model of the human skull from CT images. On the other hand, no results were extracted from that study.

1.8 Review of Studies regarding Head, and Brain Size

FE models of the human head today are often average models such as 50th percentile male with a fixed mesh density. Anthropometric data show, on the other hand, that the size of the human head varies quite a lot. It has been shown that the the length of the head of the adult varies from about 165 mm for the 5th percentile woman to about 210 mm for the 95th percentile man (Pheasant, 1996), in the Northern European population. The same difference can also be seen for the width and the height. Obviously, by including infants and other populations in the study, the variation is even greater.

A few studies have been performed regarding the size of the human head. In a study of cerebral concussion using subhuman primates, Ommaya *et al.* (1967) evaluated Holbourn's scaling law in an effort to scale thresholds from primates to a concussion threshold for humans.

Holbourn's scaling law may be written as:

$$\alpha_p = \alpha_m \left(\frac{M_m}{M_p} \right)^{2/3} \qquad (1.4)$$

where, α_p is the angular acceleration threshold for the prototype (man), and α_m is the angular threshold for the animal model. It states that an angular injury threshold for a species can be scaled from a known angular threshold for a different species, simply by using the mass ratio of the brains.

Krauland *et al.* (1981) used superior halves of 25 cadaver heads, and applied horizontal plane rotational accelerations of 2.25-9.32 krad/s^2, with durations of 8-28ms. The results showed relative motion between the skull and the brain of up to 2cm in magnitude. It was also shown that the relative motion increased with increasing age and degree of brain atrophy (decreased brain size). Also the relative motion increased with increasing magnitude of the angular acceleration.

Margulies *et al.* (1985) showed that the peak shear strain in a 2D gel model increased with size according to Holbourns scaling law. Margulies and Thibault (1992) used an infinite cylinder approximation and a centroidal load application to extrapolate data from non-centroidal loads

producing moderate to severe DAI in baboons to derive a DAI tolerance criterion for humans. The applied angular pulse were scaled to produce the same shear strain in the central parts of the cylinders with radie=6.2cm (human approximation) as for the cylinder with radie=3.2cm (for the baboon). In that study, it was also found that the maximum shear strain in the central parts of the cylinder increased with increasing size.

In a two-dimensional (2D) numerical study by Prange *et al.* (1999), coronal rotational accelerations were used to evaluate differences in intracranial responses between adults and children. Prange *et al.* (1999) scaled geometry and material properties in a 2D coronal cross-section to model an adult and a child (two weeks old). It was found that the adult model suffered more than twice the amount of (principal) strain in the central parts of the brain compared to the child model when applying an impulse with a peak angular acceleration of 1167 r/s^2 and angular velocity of 43.7 r/s. However, the adult brain tissue was assumed to be about half as stiff as the child's.

1.9 Review of Studies regarding Head Kinematics

Experimental Studies
In a pioneering work Holbourn (1943) observed shear strain patterns in 2D gel models, and also claimed that translation is not injurious, while rotation could explain the majority of traumatic brain injuries due to the nearly incompressible properties of brain tissue.

Unterharnscheidt and Higgins (1969) applied controlled angular accelerations to squirrel monkeys. The monkeys suffered subdural hematoma, torn bridging veins, and lesions of the brain and the spinal cord.

Hirch and Ommaya (1970) studied the rotational and translational rigid body motions of the head after impact in Rhesus monkeys with and without a cervical collar. When a collar was worn, the head rotations were reduced, and the animals displayed an increased tolerance to occipital impact for the onset of cerebral concussion. Although head rotations were reduced in this nonconcussed protected group, the translational motion of the head exceeded that attained by concussed monkeys not wearing collars but struck at equivalent impulse levels.

Gennarelli *et al.* (1972) subjected 25 squirrel monkeys to controlled sagittal plane head motions. It was found that in 12 of the 25 animals subjected to pure translation of the head at peak positive g levels ranging between 665-1230 g (6-8 ms duration), cerebral concussion was not obtainable. In contrast, 13 of the animals who were subjected to head rotations at peak positive tangential (at c.g.) g levels ranging between 348-1025 g (5.5-8 ms duration) were all concussed. Visible brain lesions were noted in both translated and rotated groups but with a greater frequency and severity after rotation.

Abel *et al.* (1978) studied the incidence and severity of cerebral concussion in the Rhesus monkey following sagittal plane angular acceleration. Controlled single approximately sinusoidal pulse of angular acceleration about a fixed axis perpendicular to the sagittal plane were applied. Angular acceleration values ranged up to 1.2 x 10^5 rad/sec^2, and peak values of tangential acceleration at the center of the mass of the brain reached 1300 g's. The severity of the injury correlated well with the mechanical input in terms of acceleration (angular or tangential). The occurrence of subdural hematomas originating in the parasagittal bridging veins in 16 of the experiments was well correlated with peak values of tangential acceleration with onset occurring

at values of 700 g's. The results suggested that subdural hematoma formation is as a threshold phenomenon.

Hodgson *et al.* (1979) used monkey brain hemisection models, and subjected those to translation, pure rotation and a combined motion. Linear and angular head accelerations were measured as well as brain displacement relative to the skull and shear strain at several locations. Pure rotation produced the highest, most diffuse and long lasting shear strain and brain displacement, while translation produced very low shear strain. Highest shear strain during rotation was recorded in the brainstem rather than on the periphery as many have predicted. Those results suggested that the mechanism of brainstem injury, regardless of head motion, is due to shear caused by stretching of the cervical cord.

Hodgson *et al.* (1983) studied the role of impact location in reversible cerebral concussion. Mechanical impacts were delivered to the front, side, rear and top of rigid protective caps worn by six anesthetized monkeys. These tests were to produce reversible concussion and to determine differences in tolerance to concussion among the four impact sites. Higher linear and angular accelerations produced longer periods of unconsciousness (more than 3 times) on the side than at any of the other locations. However, the decrease in concussion tolerance was accompanied by higher accelerations for side impacts.

Ono *et al.* (1980) found that the occurrence of concussion in monkeys did not correlate with rotational acceleration of the head. On the contrary, the occurrence of concussion correlated highly with the linear acceleration of the head.

Gennarelli *et al.* (1982) produced traumatic coma in monkeys (23 *Macaca mulatta* and 22 *Pabio nubis*) by accelerating the head without impact in non-centroidal sagittal rotation (posterior to anterior), non-centroidal coronal rotation, and a non-centroidal oblique motion (head turned 30 degrees from sagittal and moved posterior to anterior). A similar angular acceleration with a magnitude of $1\text{-}2 \cdot 10^5$ rad/s^2 was used for all directions. It was found that the majority of the animals that was enduring the coronal motion suffered coma lasting longer than 6 hours, while all animals that were accelerated in the sagittal plane had coma lasting less than 2 hours. Also, all the laterally injured animals had a degree of DAI in the corpus callosum and superior cerebellar peduncle similar to that found in severe human head injury. This was further studied by Gennarelli *et al.* (1987). Three groups of 13 monkeys were subjected to non-centroidal sagittal and coronal angular accelerations as well as a centroidal horizontal plane rotation. Again, the longest coma was found for the coronal impulse, while the shortest coma was found for the sagittal direction. Brain stem damage was seen almost exclusively in the animals subjected to the non-centroidal coronal acceleration. The sagittal plane motion showed either axonal damage confined to the cerebral hemispheres or no traces of DAI, while the horizontal impulse produced almost exclusively DAI in the central parts of the brain. The coronal impulse, on the other hand produced DAI in both the bran stem and the corpus callosum.

Numerical Studies

Ward and Chan (1980) developed a 3D FE model of a primate head. The model was subjected to the sagittal plane, non-centroidal, and biphasic angular acceleration pulse reported in previous experiments on a Rhesus monkey (Abel *et al.*, 1978). They found that the maximal shear stresses were around 50% lower when simulating without applying the rotational component of the acceleration.

Lee *et al.* (1987) used a 2D sagittal model, and Huang *et al.* (1999) used a coarsly meshed (1300 elements) 3D model (previously presented in Shugar, 1977) to study the mechanisms of SDH. They found that the contribution of angular acceleration to tearing of bridging veins was greater than the translational acceleration. However, the bridging veins were not modeled, and tied interfaces between the skull and the brain were used. Instead, an indirect approach was used; The observed change in distance between a node in the interior of the skull and a node in the brain, located close to the vertex, was used as a measure of bridging vein deformation.

Chu *et al.* (1994) used a 2D parasagittal FE model, and found the magnitude of shear stress and pressure to be almost independent of the direction in a sagittal motion. A later 3D study was performed by Huang *et al.* (2000), which presented similar results. However, in both studies, a tied interface between the skull and the brain was used. Also, in the 3D study by Huang *et al.* (2000), the middle fossae and the sphenoid ridge was not modeled, and in the 2D study by Chu *et al.* (1994), the Petrous bone was omitted from the model. In reality, simulating gliding contusions would require a detailed skullbase, as well as a way of including the potential relative motion between the skull and the brain.

Bandak and Eppinger (1994) presented the Cumulative Strain Damage Measure (CSDM), which is equal to the cumulative volume fraction of the brain that has experienced a specific level of maximal principal strain. They used a previously developed 3D FE model of the human head (DiMasi *et al.*, 1991), and subjected it to various pulses of sagittal and coronal plane centroidal and a noncentroidal angular velocities, as well as translational acceleration pulses in the anterior posterior direction. It was suggested that translation impulses had little influence on CSDM. However, the translational acceleration was adjusted to give an equal acceleration experienced at the c.g. of the head compared to the noncentroidal impuls. The noncentroidal rotational impulse was a rotation around an axis 300mm below the c.g. In this study, it was also found that the sagittal plane rotation produced a larger CSDM than a corresponding coronal, which is contradicting results obtained in earlier animal experiments (Gennarelli *et al.*, 1982, 1987).

DiMasi *et al.* (1995) used the kinematics from a Hybrid III dummy in a crash test in which a Hybrid III dummy impacted an A-pillar. The crash test was simulated using the full kinematics, only the rotational motion, and the translational kinematics only. It was found a higher CSDM in pure rotation, than a pure translation, while a combination of the full kinematics gave the highest values.

At the same time, Ueno and Melvin (1995) did a similar study, also using the kinematics from a Hybrid III dummy, but applying it to a 2D head model. They found that the use of either translation or rotation alone may underestimate the severity of an injury. The results also indicated that translational acceleration is related to pressure while rotational acceleration has a dominant effect on shear deformation. However, the nodes at the skull-brain boundary was rigidly connected.

Zhou *et al.* (1995) found higher strain in the bridging veins during the acceleration than in deceleration phase while applying the acceleration pulse from Abel *et al.* (1978). Since the acceleration pulse is directed in the posterior-anterior direction, it is suggested that SDH is easily produced in an occipital impact than a corresponding frontal one.

Later, the same researchers (Zhou *et al.*, 1996) scaled the impulse by Abel *et al.* (1978) to a corresponding impulse for humans using Holbourn's scaling law. This impulse was applied to a sagittal rotation and a coronal rotation. It was found that sagittal motion causes higher strain in

the bridging veins than a corresponding coronal. Also, higher stresses in the brain were found for the coronal impulse. However, more than four times higher shear stresses was found in the corpus callosum for the sagittal impulse compared with an identical sagittal pulse. Although showing encouraging results, both studies utilized a tied interface between the skull and the brain, which is unlikely to allow any large relative motion.

Zhang *et al.* (2001) compared brain responses between frontal and lateral impacts, and found higher shear stress in the core of the brain during a lateral impact. This confirmed earlier results by Gennarelli *et al.* (1982) that loads in the lateral direction are more likely to cause DAI compared to impulses in the sagittal plane. However, a tied interface was imposed between the skull and the brain leaving out any possibility of evaluating relative motion induced injuries such as Subdural Hematoma (SDH).

2 Numerical Methods

The biomechanics of the human head can be seen as a brain movement within an externally loaded skull and this gives a complex three dimensional dynamic boundary value problem. The internal biomechanical responses of the brain cannot be completely measured by experimental techniques. Analytical models are limited to problems with regular geometry, simple boundary conditions and homogeneous material properties. Numerical approaches, on the other hand, approximate the analytical solution with a numerical procedure. The finite element method (FEM) is superior to other numerical methods. Geometrically complex material domains of the problem can be represented by a collection of geometrically simple sub domains called Finite Elements. The approximation functions are then derived over each finite element, since any continuous function can be represented by a linear combination of algebraic polynomials. This can be viewed as a piece wise application of the variational methods, in which the approximation functions are algebraic polynomials. Head injuries are related to tissue material failure, characterized in some form of stress, strain or deformation. Finite element analysis can provide stress, strain or deformation distributions across, and within the different tissues for a given biomechanical input, such as a head motion or head impact. Identifying magnitudes and location of the quantities at which the tolerance level of the tissue is exceeded provides the link between the external mechanical quantities and the internal injuries. Finite element models are repeatable and reproducible, and simulations can be seen as surrogate experiments without biological variability. They can also include irregular geometry, inhomogeneous and nonlinear material properties and complex boundary and loading conditions.

Numerical methods like the Finite Element Method (FEM) have been used for the last 30 years as an engineering tool in the mechanical design process. In the biomechanical field, numerical techniques were first used to complement experimental car crash simulations. Today, the numerical technique has reached such a level that complex structures like the human being can be modeled with good accuracy. However, much research remains to be done before a complete model of the human being can be presented. Here, a brief introduction is given to a dynamic finite element code. The theory presented in this chapter is covered in a more rigorous manner by Hallquist (1998), Bathe (1996), and Belytschko *et al.* (2000).

2.1 Theory of Explicit Finite Element Programs

In this study, the FE code LS-DYNA3D has been used (Hallquist, 1998). LS-DYNA3D is a non-linear explicit 3D-Finite Element code for analyzing large deformation dynamic responses of deformable and rigid structures. A Lagrangian formulation is used and the equations of motion for a continuum in time are solved by the central difference method. The program is well suited to crash simulations as it has well working contact algorithms that permits gaps and sliding with friction.

A dynamic calculation is divided into a sequence of time steps. For each time step the displacement vector is calculated. The kinematic behavior is computed by solving the momentum equation (Eqn. 2.1) of the system,

$$\sigma_{ij,j} + \rho f_i = \rho \ddot{u}_i \qquad (2.1)$$

where σ is the Cauchy stress tensor, f_i is the body force vector per unit mass, u is the displacement and ρ is the density.

By using interpolation functions (N_α^e) for the nodes and setting the virtual work equal to zero, we obtain a system of ordinary differential equation:

$$M\ddot{r} = F^E - F^I \tag{2.2}$$

where M is the mass matrix, r is the nodal displacement vector, F^I is the internal nodal force vector, and F^E is the external nodal load vector.

$$\mathbf{F}^I = \sum_{e=1}^{N_e} \left[\int_{v_e} \sigma_{ij} \frac{\partial N_\alpha^e}{\partial x_j} dv_e \right] \tag{2.3}$$

$$\mathbf{F}^E = \sum_{e=1}^{N_e} \left[\int_{v_e} \rho f_i N_\alpha dv_e + \int_{s_e} t_i N_\alpha ds_e \right] \tag{2.4}$$

$$M\ddot{r} = \sum_{e=1}^{N_e} \left[\int_{v_e} \rho N_\alpha N_\beta dv_e \right] \ddot{x}_{\beta_i} \tag{2.5}$$

where N^e is the number of elements, v_e is the element volume.

2.2 Time integration

Equation 2.2, is solved in the time domain by explicit integration using the central difference method (Eqn 2.6-2.8). For explicit programs, the equation of motion is evaluated at the old time step t^n.

$$\ddot{r}^n = M^{-1}\left(F^E - F^I\right) \tag{2.6}$$

$$\dot{r}^{n+1/2} = \dot{r}^{n-1/2} + \ddot{r}^n \Delta t^n \tag{2.7}$$

$$r^{n+1} = r^n + \dot{r}^{n+1/2} \Delta t^{n+1/2} \tag{2.8}$$

where Δt^n is the time step at time n and

$$\Delta t^{n+1/2} = \frac{\Delta t^n + \Delta t^{n+1}}{2} \tag{2.9}$$

The geometry is updated by adding the total displacements to the initial geometry

$$\mathbf{x}^{n+1} = \mathbf{x}^0 + \mathbf{r}^{n+1} \tag{2.10}$$

The above scheme is repeated from time zero to the chosen termination time. The time step used depends on the size of the elements and the material properties. The smallest time step is computed based on an estimate of the highest eigenvalue of each element. It needs to be small enough to maintain a stable solution. The time step for a beam can be calculated by:

$$\Delta t = \frac{L}{\sqrt{E/\rho}} \tag{2.11}$$

where L is the length of the beam (element), E is the Young's modulus and ρ is the density.

2.3 Mooney-Rivlin Hyperelasticity for Brain Tissue

Stresses for elastic and hyperelastic materials are path independent. Hyperelasticity or Green elasticity is path-independent and fully reversible, and the stress is derived from a strain energy potential. It can be shown (Malvern, 1969) that the stored strain energy for a hyperelastic material which is isotropic with respect to the initial, unstressed configuration can be written as a function of the principal invariants (I_1, I_2, I_3) of the right Cauchy-Green deformation tensor, i.e., $W=W(I_1,I_2,I_3)$. Mooney and Rivlin showed that the simple form

$$W(I_1, I_2) = C_{10}(I_1 - 3) + C_{01}(I_2 - 3) \tag{2.12}$$

Closely matches results from large deformation experiments on incompressible rubber.

The theory of hyperelasticity is well known and the reader is referred to Holzapfel (2000) and Ogden (1984) for more details. To accommodate large elastic deformations, a Mooney-Rivlin hyperelastic constitutive law (Ogden, 1984) was used for tissues of the central nervous system (CNS). A homogeneous, isotropic, and non-linear constitutive model was based on the work by Mendis *et al.* (1995), who derived the Mooney-Rivlin parameters using experiments published by Estes and McElhaney (1970) on white matter from the corona radiata region. In addition, dissipative effects were taken into account through linear viscoelasticity by introducing a viscous stress, which is linearly related to the elastic stress.

$$C_{10}(t) = 0.9C_{01}(t) = 620.5 + 1930e^{-t/0.008} + 1103e^{-t/0.15}(Pa) \tag{2.13}$$

where C_{10} and C_{01} are the Mooney-Rivlin constants. This law cannot be implemented directly in LS-Dyna (LSTC, 2001). Instead, the linear viscoelasticity is expressed in terms of a prony series with shear moduli G_i, and time decay constants β_i, representing Maxwell elements in which viscous stresses are added to those determined from the strain energy function. Using the relationship $G=2(C_{10}+C_{01})$ gives the values of the shear moduli.

Nearly Incompressible material modeling

In a conventional FE formulation, severe numerical difficulties are encountered for nearly incompressible materials because small volumetric strains cause large hydrostatic pressures due to the high effective bulk modulus. To circumvent this problem a displacement-pressure (u/p) finite element formulation is used. This procedure features replacement of the pressure computed from the diplacement field by a separately interpolated pressure. To take into account the

compressibility, a hydrostatic work term, $W_H(J)$, is included in the strain energy functional in Eq. *(2.12)* which is a function of the relative volume, J (Ogden, 1984):

$$W(J_1, J_2, J) = C_{10}(J_1 - 3) + C_{01}(J_2 - 3) + W_H(J) \qquad (2.14)$$
$$J_1 = I_1 J^{-1/3}$$
$$J_2 = I_2 J^{-2/3}$$

In order to prevent volumetric work from contributing to the hydrostatic work, the first and second strain invariants are modified as shown. This procedure is described more in detail by Sussman and Bathe (1987).

3 Discussion

The present thesis shows that the number of head injuries in Sweden is still very high. Although the majority of the cases belong to the mild group, the negative consequences for the individual, relatives and the society as a whole are unacceptable. Thus, in order to reduce the number of head injuries, further actions have to be taken. One such action is the development of a FE model for further analysis of impact consequences in an effort to find preventive strategies.

As seen in paper A, the incidence of hematoma cases in Sweden has increased with a relatively steady rate the last 14 years. At the same time, an increasing number of head injuries among people older than 65 years of age is seen. It is also shown that an elderly patient with hematoma is more likely to have a long hospital stay. This information gives an increased interest to the results presented in paper C.

In paper C, it was found that by reducing the brain size and thereby increasing the volume in the subdural space in the FE model, a significant increase in relative motion between the skull and brain occurred, which correlated with the reduction of brain size. This has never been studied in detail before. Krauland *et al.* (1981) used superior halves of 25 cadaver heads, and applied horizontal plane rotational accelerations. In that study, it was shown that the relative motion between the skull and the brain increased with increasing age and degree of brain atrophy (decreased brain size), which supports the findings of paper C. However, only angular acceleration pulses in the axial direction was imposed. Also, the importance of impact directions in causing SDH is supported by previous studies. Hirakawa *et al.* (1972) studied 309 adult cases of chronic SDH, and found that sagittal blows were the dominant causes. They also found that 9 out of 27 cases of SDH due to sport accidents were caused by judo, and "they fell down on their back". The importance of impact direction in causing SDH was studied by Fruin *et al.* (1984) in their clinical study of interhemispheric SDH. They found that six out of eight cases with known trauma sites were due to occipital impacts, which supports an earlier study by Jamieson and Yelland (1972), who found that axial (*frontal, occipital, or vertical according to their definition*) trauma sites were accounting for more than half of the simple subdural hematomas. The complicated hematomas were, on the other hand, slightly over represented by lateral trauma sites. Further on, the clinical studies by Hirakawa *et al*. (1972) and Jamieson and Yelland (1972) both reported SDH to be found scarcely in the occipital region, which supports that the largest strains were found for the centrally or frontally located bridging veins for all impact directions in both paper C and D. Zhou *et al.* (1995) found higher strain in the bridging veins during the acceleration than in the deceleration phase while applying the acceleration pulse from Abel *et al.* (1978). Since the acceleration pulse is directed in the posterior-anterior direction, it is suggested that SDH is more easily produced in an occipital impact than in a corresponding frontal one. Later, the same researchers (Zhou *et al.*, 1996) scaled the impulse by Abel *et al.* (1978) to a corresponding impulse for humans using Holbourn's scaling law. This impulse was applied to a sagittal and coronal rotation. It was found that sagittal motion causes higher strain in the bridging veins than a corresponding coronal motion. However, both studies utilized a tied interface between the skull and the brain, which is unlikely to allow any large relative motion between the skull and the brain. This questions the validity of these results, since the strain observed in the bridging veins is highly dependent on the amount of relative motion.

The size of the human head varies within a large range. The parametrized geometry of the model utilizes a tool for studying the effects of these variations. Variational studies of intracranial

pressures and deformations can be performed. Based on this model, new head injury criteria can be evaluated for adult males and adult females within certain percentiles, when it comes to geometry. In this way, the criteria are valid for a larger span of the population. Today, most FE models of the human head are based on the geometry of an average adult male and, as indicated by the anthropometric study, the worst case might not lie within the 50th percentile.

Paper B shows that it is possible to parameterize the 3D geometry of the human head. It is also possible to obtain a variable element mesh density of such an FE model. The spatial coordinates of points on the boundaries of the different tissues were scaled respectively in the same manner as described by Mertz *et al.* (1989). The inner and outer surfaces of the skull were scaled individually. In this way, a detailed and parametrized model of the human head was created, which can be scaled with respect to the width, length, height and thickness of the skull as well as the overall size of the head and neck. A non-linear and viscoelastic constitutive law together with a displacement-pressure element formulation for the CNS tissues gives reasonably good correlation with experiments.

Numerous FE models of the human head (Zhou *et al.*, 1995, Ruan *et al.*, 1997, Claessens *et al.*, 1997, Kuijpers *et al.*, 1995, among others), have been validated against the experiments of Nahum *et al.* (1977). These models and other "state of the art" 3D FE models of the human head have all assumed isotropic, linear elastic or linear viscoelastic and homogeneous material properties within each modeled component. Biological materials do not follow the constitutive relations for common engineering materials. A biological material is often anisotropic, inhomogeneous, nonlinear and viscoelastic. In addition, there is a great variability between different individuals. Isotropic material properties is an approximation which can be justified for most of the components but orthotropic properties can be used for fibrous materials without a measurable increase in computational cost. The assumption of linear elasticity or viscoelasticity is a great limitation, especially in CNS tissue modeling due to its typical nonlinear behavior and also because it is often enduring large deformations during impacts and accelerations of the head. Thus, a hyperelastic and viscoelastic constitutive law was used. In combination with the incompressible finite element formulation, this gives a good correlation between experiments and simulations. To further increase accuracy, the actual geometry of the specimen (overall length, width and height) was reproduced according to the measurements of Nahum *et al.* (1977). To increase the duration of the impact, Nahum *et al.* placed various paddings between the impactor and the scalp. The geometry and size of the impactor (6' cylindrical load cell), and the approximate thickness and type of padding material was found and modeled. In a previous study by Ruan *et al.* (1997), they adjusted the material properties of the skull to get the right impact duration.

Bradshaw and Morfey (2001) concluded that it is not acceptable to validate FE models for pressure and then use them for injury prediction. This is especially evident since tissue level models (Bain *et al.*, 2000) have shown that diffuse axonal injury (DAI) is a function of distortional strain, and not dilatation (pressure). A more relevant parameter for validation of a FE model of the human head should therefore be strain. Such data does not exist, but since strain (as in the Lagrangian definition) is a function of the deformation gradient, an indirect approach can be used. Validation against relative displacement between the brain and skull, as described in paper E, should therefore be a better indicator of the injury prediction capabilities of an FE model of the human head. If the relative displacement data are continuous and differentiable (as in this case), correlation of relative motion in spatial coordinates will indicate a correlation of strain between empirical and numerical results.

The results from the study in paper D showed smaller differences between rotational and translational impulses than expected when looking at previous studies. However, when comparison between translation and rotation has been performed, the usual approach has been to compare a non-centroidal rotational impulse with a translational impulse giving a similar acceleration measured at the c.g. (Margulies *et al.*, 1985, Bandak and Eppinger, 1994). This give a good basis for evaluation of the effects of a pure translation in comparison with a translation plus a rotation for criticism of head injury criteria based solely on the translational acceleration. However, in this case the comparison will be between a translational impulse, and an equal translational impulse in addition to the induced rotational one. A more objective approach could be to apply the same dosage of mechanical energy per time unit (*i.e. the power*) for the separate degrees of freedom, as described in paper D, and proposed as a new head injury criteria: *the head impact power* (Newman *et al.*, 2000). Gennarelli *et al.* (1972) subjected 25 squirrel monkeys to controlled sagittal plane head motions, and found brain lesions in both translated and rotated groups but with a greater frequency and severity after rotation. Studies by DiMasi *et al.* (1995), and Ueno and Melvin (1995) found that the use of either translation or rotation alone may underestimate the severity of an injury. This support the findings in paper D of only 40-100% larger shear strains in the central parts of the brain for a pure rotation compared to a translation with the same impact power. However, only a slight increase in the strain suffered by the CNS tissue might alter the outcome of a trauma. Bain and Meaney (2000) estimated a tissue threshold for axonal damage to a Lagrangian principal strain of about 0.2 in experiments on optic nerves of guinea pigs. The findings of high strain in the central parts of the brain and lower strains in the brain stem for the axial rotational impulse in paper D supports the findings of Gennarelli *et al*. (1987) that the horizontal impulses produced almost exclusively DAI in the central parts of the brain.

Ono *et al.* (1980) found that the occurrence of concussion in monkeys correlated highly with the linear translational acceleration of the head and not with the rotational acceleration. The results presented in paper D do not support those findings, since areas associated with diffuse injuries, endured higher stresses and strains for a rotational impulse compared to a translational one with the same impact power. A possible explanation for this difference is the experimental approach used, which involved large displacements of the head relative to the chest. This might have induced stretching of the upper part of the spinal cord and the brain stem. This stretching of the brain stem has previously been discussed in Hodgson *et al.* (1979), who suggested that the mechanism of brainstem injury, regardless of head motion, is due to shear caused by stretching of the cervical cord. This, might also explain the occurrence of higher shear strain in the brain stem for the superior-inferior (SI), and the IS translational impulses, since the upper part of the spinal cord, and thus the lower part of the brain stem is likely to endure large inertia forces when accelerated in the axial direction.

Zhou *et al.*, (1996) scaled the impulse by Abel *et al.* (1978) to a corresponding impulse for humans using Holbourn's scaling law. This impulse was applied to a sagittal rotation and a coronal rotation. Higher stresses in the brain were found for the coronal impulse. However, more than four times higher shear stress was found in the corpus callosum for the sagittal impulse compared with an identical sagittal pulse. Later, Zhang *et al.* (2001) compared brain responses between frontal and lateral impacts, and found higher shear stress in the core of the brain during a lateral impact. This confirmed earlier results, by Gennarelli *et al.* (1982, 1987), that loads in the lateral direction are more likely to cause DAI compared to impulses in the sagittal plane.

Although showing encouraging results, both these studies utilized a tied interface between the skull and the brain, which questions the reliability of these results since it is unlikely that any

significant relative motion between the skull and the brain can be simulated using such a modeling technique when imposing a large amount of impact energy.

The skull-brain interface contains, in addition to CSF, also bridging veins and arachnoidal trabeculations that limit this interface in the radial direction and motivates usage of a tied interface. This can explain the experimental correlation for the frontal pressure when utilizing a tied interface. For large rotational loads, on the other hand, a contact definition that can transfer loads in tension as well as permit large relative motion between the skull and the brain should be preferred.

The technique adopted when utilizing the sliding only interface (paper C) has some limitations. When simulating the experiments, small penetrations of the brain through the CSF occurs for shorter duration of the simulations. This might have caused a slight increase in the relative motion. In the distributed parameter algorithm, any intrusion of the slave surface into the master surface is ignored. Thus, an over penetration might be present in high pressure areas. This gives an indirect way of simulating a local "flow" from high pressure areas. This approach is not verified, and Eulerian methods including advection of material for the CSF should be preferred. Although, a correlation was found between the model and previously reported experiments on relative motion magnitude (Al-Bsharat *et al.*, 1999) in paper C, it is concluded that more effort is needed to look into fluid-structure interaction techniques.

Huang *et al.* (1999, 2000) used a coarse mesh with a mesh density approximately the same to that shown in Fig. 3 (left), in chapter 1.4. The accuracy of an FE model is (up to a certain point) significantly dependent on its discretisation. In this case, it is important that the FE model describes the complex geometry of the human head. It depends on how many elements are used to describe the complex boundaries and surfaces. In the future when the computer speed increases, further improvements can be done with this model because the mapped meshing gives a flexible number of elements.

4 Conclusions

A detailed and parameterized FE model of the human head was developed and used to evaluate the effects of head size, brain size and impact directions. The most important conclusions from the studies reported in papers A-E is listed below.

Paper A

- Head injuries attributable to transportation accidents decreased, while falls caused an increasing proportion of head injuries.
- An increase in head injuries among elderly was observed, and primary prevention strategies may need to be targeted at this age group, and at preventing falls.
- Concussions and fractures decreased over time. Diffuse or focal injures showed a steady rate of occurrence over the study interval while hematoma cases increased.

Paper B

- The maximal effective stresses in the brain increased with increasing head size when applying the same acceleration impulse or when impacting the head towards padded surfaces using the same velocity.
- The size dependence of the intracranial stresses associated with injury is not predicted by the HIC.

Paper C

- The increased risk of SDH in elderly people may to a part be explained by the reduced brain size resulting in a larger relative motion between the skull and the brain with distension of bridging veins.
- The consequences of this increased relative motion due to brain atrophy cannot be predicted by existing injury criteria.
- More effort is needed to understand the mathematics of fluid-structure interfaces when these are utilised for the skull-brain interface.

Paper D

- The highest shear strain in the brain stem is found for the SI translational impulse, and in the corpus callosum for the lateral rotational impulse when imposing acceleration pulses corresponding to the same impact power.
- HIC is unable to predict the consequences of a pure rotational impulse, while HIP needs individual scaling coefficients for the different terms to account for the difference in load direction.
- It is also suggested that a further evaluation of synergic effects of the directional terms of the HIP is necessary to include combined terms and to improve the injury prediction.

Paper E

- Localized motion of the brain is highly sensitive to the shear properties of the brain tissue.
- The results suggest that significantly lower values of the shear properties of the human brain than utilized in most 3D FE models today must be used to be able to predict the localised brain response of an impact to the human head.
- The localized motion due to low severity impacts seems to be less sensitive to the modeling approach of the skull-brain interface.
- There is a symmetry in the motion of the superior and inferior markers for both the model and the experiments following a sagittal and a coronal impact. This can possibly be explained by the nearly incompressible properties of brain tissue.
- Larger relative motion between the skull and the brain is apparent for an occipital impact than for a frontal one for both experiments and FE model. This is in line with clinical findings.
- Smaller relative motion between the skull and the brain is apparent for lateral impact than for a frontal one for both experiments and FE model. This is thought to be due to the supporting structure of the falx cerebri.
- Pressure seems to be more sensitive to the skull-brain interface than to the constitutive parameters chosen for the brain tissue.

5 Future work

The present study demonstrates the applicability of the FE method to the biomechanics of the human head. It also shows the possibility of parameterization of the geometry and the element sizes of such an FE model. However, inclusion of ventricles and differentiation between white and gray matter using more detailed surface definitions of the boundaries between them must be done.

More extensive testing of meninges and brain tissue is desired when it comes to directional and regional differences for more accurate representation of their properties. A comparison between different constitutive models for CNS tissues should also be performed, as well as a study of the structural effects of the bone marrow for the cranial bones. It is also concluded that more work is needed to understand the mathematics of the fluid-structure interaction in the human head for a proper modeling of the skull-brain interface.

Coupling of the head model with a detailed neck model including muscles and inclusion of a detailed spinal cord fitting the head and neck model is also planned.

Holbourn (1943) stated that the consequences of long duration impulses to the head (when it comes to shear strain) is proportional to the magnitude of acceleration, while short duration impulses are dependent only on the total change of velocity. This interesting hypothesis could also be explored in a rigorous manner using the head model.

By further improving the present FE model, it might be possible to use the model for (retrospectively) evaluating CNS injuries after traffic accidents. If this can been achieved, the FE model should be a powerful tool for the innovation of better preventive strategies in the traffic.

References

Abel J.M. Gennarelli T.A., Segawa H. (1978). Incidence and severity of cerebral concussion in the rhesus monkey following sagittal plane angular acceleration, 22nd Stapp Car Crash Conf, Society of Automotive Engineers, SAE Paper No. 780886.

Al-Bsharat, A.S. *et al.* (1999). Brain/Skull Relative Displacement Magnitude Due to Blunt Head Impact: New Experimental Data and Model, In 43rd Stapp Car Crash Conf., SAE Paper No. 99SC22, Society of Automotive Engineers, pages 321-332.

Anzelius, A. (1943). The effect of an impact on a spherical liquid mass. *Acta. Pathol. Microbiol. Scand., Suppl. 48,* pp. 153-159.

A.P.R. (1988). Investigation of Relationship Between Physical Parameters and Neuro-Physiological Response to Head Impact, Final Report, NHTSA Contract DTRS-57-86-C-00037.

Arbogast, K.B. *et al.* (1997). Properties of Cerebral Gray and White Matter Undergoing Large Deformation, in: *Prevention Through Biomechanics*, Symposium Proceedings, Wayne State University, pps 33-39.

Bain, B.C., Meaney, D.F. (2000). Tissue-Level Thresholds for Axonal Damage in an Experimental Model of Central Nervous System White Matter Injury. *J. Biomech. Engng*.**16**, pps 615-622.

Bandak, F.A., Eppinger, R.H. (1994). A three-dimensional FE analysis of the human brain under combined rotational and translational accelerations, in: *38th Stapp Car Crash Conf*., *Society of Automotive Engineers*, pps 145-163.

Bandak, FA *et al.* (1995). An Imaging-Based Computational and Experimental Study of Skull Fracture: Finite Element Model Development, *J Neurotrauma*, **12**(4) , pp. 679-688.

Barber, T.W., Brockaway, J.A., Moffatt, C.A. (1970). Static compression testing of specimens from an embalmed human skull. Texas Reports on Biology and Medicine, **28**(4): 497-508.

Bathe, K.J. (1996). Finite element procedures. Prentice Hall, New Jersey.

Belytschko, T., Kam Liu, W., Moran, B. (2000). Nonlinear Finite Elements for Continua and Structures. John Wiley & Sons Ltd., West Sussex, England.

Chan, H.S. (1974). Mathematical model for closed head impact, in*: 18th Stapp Car Crash Conf, Society of Automotive Engineers,* pages 557-579.

Cheng L.Y. *et al.* (1990). Finite Element Analysis of Diffuse Axonal Injury, inVehicle Crashworthiness and Occupant Protection in Frontal Collisions, SAE Paper No. 900547, Society of Automotive Engineers.

Claessens, M., Sauren, F., Wismans, J. (1997). Modeling of the Human Head Under Impact Conditions: A Parametric Study, in*: 41st Stapp Car Crash Conf*, SAE Paper No. 973338, Society of Automotive Engineers, pps 315-328.

Cooper P.R. (1982). Post-traumatic intracranial mass lesions, in *Head injury,* Williams and Wilkins, Baltimore/London. Pp. 185-232.

Department of Transportation (DOT), National Highway Traffic Safety Administration (1972). *Occupant Crash Protection – Head Injury Criterion S6.2 of MVSS 571.208,* Docket 69-7, Notice 17. NHTSA, Washington, DC.

DiMasi, F. *et al.* (1991). Simulated head impacts with upper interior structures using rigid and anatomic brain models, in Auto and trafic safety., No. 1, Ed. R. Strombotne, National Highway Traffic Safety Publication, Vol. 1.

DiMasi, F. *et al.* (1995). Computational analysis of head impact response under car crash loadings, in*: 39th Stapp Car Crash Conf, Society of Automotive Engineers,* SAE Paper No. 952718*,* pp. 425-438.

Donnelly, B.R., Medige, J. (1997). Shear properties of human brain tissue. *J. Biomechanical Engineering,* **119**, pp. 423-432.

Donnelly, B.R. (1998). Brain tissue material properties: A comparison of results. *Biomechanical research: Experimental and computational, Proc. Of the 26th int. Workshop.,* pp. 47-57.

Eiband, A.M. Human Tolerance to Rapidly Applied Accelerations: A Summary of the Literature. NASA Memo 5-19-59 E.

Eppinger, R. *et al.*, (2000). Supplement: Development of Improved Injury Criteria for the Assessment of Advanced Automotive Restraint Systems-II. National Highway Traffic Safety Administration.http://www-nrd.nhtsa.dot.gov/pdf/nrd-11/Airbags/finalrule_all.pdf

Estes M. S. and McElhaney, J.H. (1970). Response of Brain Tissue to Compressive Loading. ASME paper no. 70-BHF-13.

Fallenstein, G.T. *et al.* (1969). Dynamic mechanical properties of human brain tissue. *J. Biomech.*, **2**, pp. 217-226.

Fitzgerald, E.R., Ferry, J.D. (1953). Methods for determining the dynamic behavior of gels and solids at audio frequencies: Comparison of mechanical and electrical properties, *J. Colloid Sci.,* **8**, pp.1-34.

Fruin, A.H., Juhl, G.L., Taylon, C. (1984). Interhemispheric subdural hematoma. J. Neurosurg. **60**, 1300-1302.

Gadd, G.W. (1966). Use of a Weighted-Impulse Criterion for Estimation Injury Hazard, SAE Paper No. 660793, in: *10th Stapp Car Crash Conf.*, Society of Automotive Engineers, pps 164-174.

Galford, J.E., McElhaney, J.H. (1970). A viscoelastic study of scalp, brain, and dura. *J. Biomech.,* **3**, pp. 211-221.

Gennarelli, T.A., Thibault, L.E., Ommaya, A.K. (1972). Pathophysiological Responses to Rotational and Translational Accelerations of the Head, SAE Paper No. 720970, in: *16th Stapp Car Crash Conf.*, Society of Automotive Engineers, pp. 296-308.

Gennarelli, T.A.(1981). Mechanistic approach to head injuries: clinical and experimental studies of the important types of injury, Ed. Ommaya, A.K., in Head and neck injury criteria: a consensus workshop. U.S. dept. of transportation, national highway traffic safety administration, Washington DC, pp. 20-25.

Gennarelli, T.A., Thibault, L.E. (1982). Biomechanics of acute subdural hematoma. *J. Trauma*, **22** (8), 680-686.

Gennarelli, T.A. *et al.* (1982). Diffuse Axonal Injury and Traumatic Coma in the Primate. *Ann. Neurol.* **12**, 564-574.

Gennarelli, T.A. *et al.* (1987). Directional dependence of axonal brain injury due to centroidal and non-centroidal acceleration, SAE Paper No. 872197, in: *31st Stapp Car Crash Conf.*, Society of Automotive Engineers.

Gurdjian, E.S. *et al.* (1968). Significance of relative movements of scalp, skull, and intracranial contents during impact injury of the head. *J. Neurosurgery*, **29**(1), 70-72.

Hallquist, J.O. (1998). LS-DYNA3D Theoretical Manual. Livermore Software Technology Corporation.

Hardy, W.N. *et al.* (2001). Investigation of Head Injury Mechanisms Using Neutral Density Technology and High-Speed Biplanar X-ray. SAE Paper No. 01S-52, in*: 45th Stapp Car Crash Conf.*, Society of Automotive Engineers, 337-368.

Hardy, C.H. and Marcal, P.V. (1973). Elastic analysis of a skull. ASME trans. pages 838-842.

Hirakawa, K. *et al.* (1972). Statistical analysis of chronic subdural hematoma in 309 adult cases. Neurol. Med. Chir. 12, pp. 71-83.

Hodgson, V.R., Thomas, L.M., Khalil, T.B. (1983). The Role of Impact Location in Reversible Cerebral Concussion, SAE Paper No. 831618, in*: 27th Stapp Car Crash Conf.*, Society of Automotive Engineers, 225-240.

Hodgson, V.R., Thomas, L.M. (1979). Acceleration induced shear strains in a monkey brain hemisection. SAE Paper No. 791023, in*: 23rd Stapp Car Crash Conf.*, Society of Automotive Engineers.

Holbourn, A.H.S. (1943). Mechanics of head injury. *Lancet* **2**, October 9, pp. 438-441.

Holzapfel, G.A. (2000). Nonlinear Solid Mechanics. John Wiley & Sons Ltd., West Sussex, England.

Hosey R.R. and Liu Y.K. (1981). A homeomorphic finite element model of the human head and neck, *in: Finite elements in biomechanics;* Simon B.R., Gallagher R.H., Johnson P.C. and Gross J.F. (Eds), Wiley & Son. pages 379-401.

Huang, H.M. *et al.* (1999). Three-dimensional finite element analysis of subdural hematoma. *The Journal of Trauma: Injury, Infection, and Critical Care* **47**(3), pp. 538-544

Huang, H.M. *et al.* (2000). Finite element analysis of brain contusion: an indirect impact study. *Medical & Biological Engineering & Computing* **38**(3), pp. 253-259.

Hubbard, R.P., McLeod, D.G. (1974). Definition and development of a crash dummy head. In *Proceedings of the 18th Stapp Car Crash Conf.*, SAE Paper No. 741193, Society of Automotive Engineers.

Ivarsson, J., Viano, D.C., Lövsund, P. (2001). Influence of the Anterior and Middle Cranial Fossae on Brain Kinematics During Sagittal Plane Head Rotation. *J. Crash Prevention and Injury Control.* **2**(4), pp. 271-287.

Jamieson, K.G., Yelland, J.D.N. (1972). Surgically treated traumatic subdural hematomas. J. Neurosurgery 37 (2), pp. 137-149.

Kenner V.H., Goldsmith W. (1972). Dynamic loading of a fluid filled spherical shell. Int. J. Mech. Sci, (1):557-568.

Khalil T.B. *et al.* (1974). Impact on head helmet system. IBID., (16):609-625.

Khalil T.B. and Hubbard R.P. (1977). Parametric study of head response by finite element modelling. *J Biomech*., (10):119-132.

Khalil, T.B., Viano, D.C. (1982). Critical issues in finite element modeling of head impact, SAE Paper No. 821150, in 26th *Stapp Car Crash Conf*., Society of Automotive Engineers, pp.87-102.

Kleiven, S., Peloso, P., von Holst, H. (2002). The Epidemiology of Head Injuries in Sweden From 1987 to 2000. *Submitted to Journal of Injury Control and Safety Promotion.*

Kleinberger, M. *et al.*, (1998). Development of Improved Injury Criteria for the Assessment of Advanced Automotive Restraint Systems. National Highway Traffic Safety Administration. http://www-nrd.nhtsa.dot.gov/pdf/nrd-11/airbags/criteria.pdf.

Krabbel, G. *et al.* (1995). Development of a finite element model of the human skull, *J.Neurotrauma*, Vol.12, No. 4, pp.735-742.

Krauland, W., Bratzke, H., Appel, H., Heger, A. (1981). Experimentelle neurotraumatologie - rotation. *Z. Rechtmedizin* **87** (3), 205-215.

Kuijpers, A.H.W.M. *et al*. (1995). The influence of different boundary conditions on the response of the head to impact: A two-dimensional finite element study, *J. Neurotrauma,* Vol.12, No. 4, pp. 715-724.

Kumaresan, S., *et al.* (1995), Generation of geometry of closed human head and discretisation for finite element analysis, Medical & Biological Engineering & Computing, May 1995, pp. 349-353.

Lee, M.C., Melvin, J.W., Ueno, K. (1987). Finite element analysis of traumatic subdural hematoma. In *Proceedings of the 31st Stapp Car Crash Conf.*, SAE Paper No. 872201, Society of Automotive Engineers.

Lee, M.C. and Haut, R.C. (1989). Insensitivity of tensile failure properties of human bridging veins to strain rate: Implications in biomechanics of subdural hematoma. *J. Biomech*. **22** (6/7), 537-542.

Lissner, H.R. *et al.* (1960). Experimental Studies on the Relation between Acceleration and Intracranial Pressure Changes in Man. Surgery, Gynecology and Obstetrics, September 1960, pp. 329-338.

Lövenhielm, P. (1974a). Dynamic Properties of the Parasagittal Bridging Veins. *Z. Rechtsmedizin* **74**(1), pp. 55-62.

Lövenhielm, P. (1974b). Strain tolerance of the Vv. Cerebri Sup. (bridging veins) calculated from head-on collision tests with cadavers. *Z. Rechtsmedizin* **75**(2), pp. 131-144.

Malvern, L.E. (1969). Introduction to the mechanics of a continuous medium. Englewood Cliffs, N.J. Prentice-Hall.

Margulies, S.S., Thibault, L.E., Gennarelli, T.A. (1985). A study of scaling and head injury criteria using physical model experiments. In *Proc. Of the 1985 Int. IRCOBI/AAAM Conf. On the Biomech. Of Impacts*, Göteborg, Sweden. pp. 223-235.

Margulies, S.S. Thibault, L.E. (1992). A Proposed Tolerance Criterion for Diffuse Axonal Injury in Man. *J. Biomech*. **25** (8), 917-923.

McElhaney J.H. *et al.*, 1970. Mechanical properties of cranial bone, *J. Biomechanics*. volume 3, 495 -511.

McElhaney, J.H., Roberts, V.L., Hilyard, J.F. (1976). Properties of human tissues and components: nervous tissues. In *Handbook of human tolerance*, Automobile Research Institute Inc., Tokyo, Japan, p. 143.

McElhaney, *et al.* (1973). Dynamic characteristics of the tissues of the head. In *Perspectives in Biomedical Engineering*, Kenedi, R.M., ed., MacMillan Press, London, pp. 215-222.

Melvin J.W. *et al.*, (1970). Development of a Mechanical Model of the Human Head - Determination of Tissue Properties and Synthetic Substitute Materials. 14th Stapp Car Crash Conf, Society of Automotive Engineers, SAE Paper No. 700903.

Melvin, J.W., Lighthall, J.W., Ueno, K. (1993). Brain Injury Biomechanics, in: *Accidental Injury.* Nahum, AM and Melvin, JW (eds), Springer-Verlag New York, pps. 269-290.

Melvin, J.W. (1995). Injury assessment reference values for the CRABI 6-Month Infant Dummy in a Rear-Facing Infant Restraint with Air Bag Deployment. in: *SAE International Congress and Exposition.* , SAE Paper No. 950872, Society of Automotive Engineers.

Mendis, K.K., Stalnaker, R.L., Advani, S.H. (1995). A constitutive relationship for large deformation finite element modeling of brain tissue, *J. Biomechanical Engineering*, **117** (4), 279-285.

Mertz, H.J. *et al.* (1989). Size, Weight and Biomechanical Impact Response Requirements for Adult Size Small Female and Large Male Dummies. In: SP-782-Automotive Frontal Impacts, SAE Paper No. 890756. Society of Automotive Engineers. 133 -144.

Mertz, H.J. *et al.* (1997). Inury Risk Curves for Children and Adults in Frontal and Rear Collisions. SAE Paper No. 973318. Society of Automotive Engineers. 13 -30.

Miller, R.T. *et al.* (1998). Finite Element Modeling Approaches for Predicting Injury in an Experimental Model of Severe Diffuse Axonal Injury, in: *42nd Stapp Car Crash Conf*, SAE Paper No. 983154, Society of Automotive Engineers, pps 155-166.

Miller, R.T. *et al.* (1999). Comparing experimental data to traumatic brain injury finite element models, In: *42rd Stapp Car Crash Conf*, SAE Paper No. 99SC20, Society of Automotive Engineers.

Nahum, A.M. *et al.*, (1977). Intracranial pressure dynamics during head impact. In: Proceedings of the 21st Stapp Car Crash Conf, SAE Paper No. 770922. Society of Automotive Engineers.

Newman, J.A. (1986). A Generalized Acceleration Model for Brain Injury Threshold, in: *IRCOBI Conf*. 121-131.

Newman, J.A. *et al.* (2000). A Proposed New Biomechanical Head Injury Assessment Function - The Maximum Power Index, in: *44th Stapp Car Crash Conf.,* SAE Paper No. 2000-01-SC16.

Nickell R.E., Marcal P.V. (1974). In vacuuo model dynamic response of the human skull. *J Eng. Industry*, (5):490-494.

Ogden, R.W. (1984). *Non-Linear Elastic Deformations*. DOVER PUBLICATIONS, INC., Mineola, New York.

Ommaya, A.K. *et al.* (1967). Scaling of Experimental Data on cerebral Concussion in Sub-Human Primates to Concussion Threshold for Man. In: *11th Stapp Car Crash Conf,* SAE Paper No. 670906. Society of Automotive Engineers. 73 -80.

Ommaya, A.K., Hirsch, A.E. (1971). Tolerances for Cerebral Concussion from Head Impact and Whiplash in Primates. J. Biomech, **4**, 13-21.

Ono, K. *et al.* (1980). Human head tolerance to sagittal impact reliable estimation deduced from experimental head injury using subhuman primates and human cadaver skulls. In: *24th Stapp Car Crash Conf,* SAE Paper No. 801303. Society of Automotive Engineers.

Pheasant, S., (1996). Bodyspace, Anthropometry, Ergonomics and the Design of Work, second edition. Taylor & Francis.

Pincemaille, Y. *et al.* (1989). Some New Data Related to Human Tolerance Obtained from Volunteer Boxers. SAE Paper No. 892435, in*: 33rd Stapp Car Crash Conf.*, Society of Automotive Engineers, pp. 177-190.

Prange, M.T. *et al.*, (1999). Pediatric Rotational Inertial Brain Injury: The Relative Influence of Brain Size and Mechanical Properties. SAE Paper No. 99SC23, In 43rd Stapp Car Crash Conf., Society of Automotive Engineers.

Prange, M.T. *et al.* (2000). Defining Brain Mechanical Properties: Effects of Region, Direction, and Species, SAE Paper No. 2000-01-SC15, in: *44th Stapp Car Crash Conf.,* Society of Automotive Engineers.

Pudenz, R.H., Shelden, C.H. (1946). The lucite calvarium – a method for direct observation of the brain. II. Cranial trauma and brain movement. *J. Neurosurgery* **3**, pp. 487-505.

Robbins*,* D.H., Wood, J.L. (1969). Determination of mechanical properties of the bones of the skull, *Exp. Mech.,* **9**(5), pp. 236-240.

Ruan, J.S., Khalil, T., King, A.I. (1991). Human Head Dynamic Response to Side Impact by Finite Element Modeling. *J.Biomechanical Engineering*, **113**(3), pp. 276-283.

Ruan, J.S., Khalil, T., King, A.I. (1993). Finite element modeling of direct impact. In*: 37th Stapp Car Crash Conf.*, Society of Automotive Engineers, SAE Paper No. 933114.

Ruan, J.S., Prasad, P. (1995). Coupling of a finite element head model with a lumped parameter Hybrid III dummy model: preliminary results. *J. Neurotrauma*, **12**(4), pp. 725-734.

Ruan, J.S. *et al.* (1997). Impact Head Injury Analysis Using an Explicit Finite Element Human Head Model. *J. Traffic Medicine*, **25**, 33-40.

Ruan, J.S. and Prasad, S. (2001). The Effects of Skull Thickness Variations on Human Head Dynamic Impact Responses. In*: 45th Stapp Car Crash Conf.*, Society of Automotive Engineers, 395-414.

Schueler, F. *et al.* (1994). Assessment of mechanical properties of the human skull-cap through basic biomechanical tests and quantitative computed tomography (QCT). *Proc. IRCOBI, pp. 23-37.*

Shuck, L.Z., Advani, S.H. (1972). Rheological response of human brain tissue in shear. *J. Basic Engineering*, Trans. ASME, Dec., pp. 905-911.

Shugar T.A. (1975). Transient structural response of the linear skull-brain system*. 19th Stapp Car Crash Conf*, Society of Automotive Engineers, pages 581-614.

Shugar T.A. (1977). A finite element head injury model, Vol. I: Theory, development, and results. U.S. Dept. Of Transportaton Report No. DOT-HS-289-3-550-IA.

Stalnaker, R.L. (1969), Mechanical properties of the head, Ph.D. dissertation, West Virginia University.

Stalnaker, R.L., McElhaney, J.H. (1970). Head injury tolerance for linear impacts by mechanical impedance methods. ASME paper No. 70-WA/BHF-4.

Stalnaker, R.L. *et al.* (1971). MSC tolerance curve for human heads to impact. ASME paper No. 71-WA/BHF-10.

Stalnaker, R.L. *et al.* (1987). Translational energy criteria and its correlation with head injury in the sub-human primate. *Proc. IRCOBI,* pp. 223-238.

Sussman, T., Bathe, K.J., 1987. A Finite Element formulation for Nonlinear Incompressible elastic and inelastic analysis. Computers & Structures. **26**(1/2), pp. 357-409.

Turquier, F. *et al*. (1996), Validation Study of a 3D Finite Element Head Model Against Experimental Data, in *40th Stapp Car Crash Conf*, SAE Paper No. 962431, Society of Automotive Engineers, 283-294.

Ueno, K., Melvin, J.W. (1995). Finite element model study of head impact based on hybrid III head acceleration: The effects of rotational and translational acceleration. *J. Biomechanical Engineering.* **117**(3), pp. 319-328.

Ueno, K. *et al.* (1989). Two-dimensional Finite Element Analysis of Human brain Impact Responses: Application of a Scaling Law. BED Vol. 13, ASME, pp. 123-124.

Ueno, K. *et al.* (1995). Development of Tissue Level Brain Injury Criteria by Finite Element Analysis. *J. Neurotrauma.* **12**(4), pp. 695-706.

Unterharnscheidt, F., Higgins, L.S. (1969). Traumatic Lesions of Brain and Spinal Cord due to Nondeforming Angular acceleration of the Head. Texas Reports on Biology and Medicine, **27**(1): 127-166.

U.S. National Library of Medicine, National Institutes of Health (NIH), Department of Health & Human Services, "Visible Human Database" www.nlm.nih.gov/research/visible/visible_human.html

Versace, J. (1971). A Review of the Severity Index, in: *15th Stapp Car Crash Conference*, SAE Technical paper No. 710881, 771-796.

Viano, D.C. and Lau, I.V. (1988). A Viscous Tolerance Criterion for Soft Tissue Injury Assessment. J. Biomech, **21**(5), 387-399.

Viano, D.C. (1988). Biomechanics of head injury – toward a theory linking head dynamic motion, brain tissue deformation and neural trauma, in *32nd Stapp Car Crash Conf.*, Society of Automotive Engineers, SAE Technical paper No. 881708.

.

Viano, D.C. *et al.* (1996). Simulation of Brain Kinematics in Closed-head Impact. *Int. J. of Crashwothiness*, **1**(4), 413-427.

Vrijhoef, M.M., Driessens, F.C. (1971). On the interaction between specimen and testing machine in mechanical testing procedures. *J. Biomech*, Jul 4:233-8.

Voigt, G.E. Lange, W. (1971). Simulation of head-on collision with unrestrained front seat passengers and different instrument panels, in: *15th Stapp Car Crash Conference*, SAE Technical paper No. 710863, 466-488.

Voo, L. *et al.* (1996). Finite element models of the human head. *J. Medical & Biological Engineering & Computing*, Sept. 1996, pp. 375-381.

Ward, C., Chan, M. (1980). Rotation generated shear strains in the brain. In *Proc. Of the 8th annual Int. Workshop on Human Subjects for Biomechanical Research,* Troy, MI, USA.

Ward, C.C. (1982). Finite element models of the head and their use in brain injury research. *26th Stapp Car Crash Conf,* Society of Automotive Engineers, pages 71-85.

Willinger, R. *et al.* (1992). Modal analysis of a finite element model of the head, in: *IRCOBI Conf*., Verona, 283-297.

Willinger, R. *et al.* (1995). From the finite element model to the physical model, in: *IRCOBI Conf*., Brunnen, 245-260.

Willinger, R. *et al.* (1999). Three-Dimensional Human Head Finite-Element Model Validation Against Two Experimental Impacts. *Annals of Biomedical Engng.* **27**, 403-410.

Wood, J.L. (1971). Dynamic response of human cranial bone, *J. Biomechanics*, **4** (3), pp.1-12.

Zhang, L. *et al.* (2001a). Comparison of Brain Responses Between Frontal and Lateral Impacts by Finite Element Modeling. *J. Neurotrauma*, **18** (1), 21-30.

Zhang, L. *et al.* (2001b). Recent Advances in Brain Injury Research: A New Human Head Model Development and Validation. In*: 45th Stapp Car Crash Conf.*, Society of Automotive Engineers, 369-394.

Zhivoderov, N.N. *et al.* (1982), Mechanical properties of the dura mater of the human brain. Original title: Mekhanicheskie svoistva tverdoi mozgovoi obolochki golovnogo mozga cheeloveka (Russian), *Sudebno-Meditsinskaia Ekspertiza*, **26** (1), pp. 36-37.

Zhou, C. *et al.* (1995). A new model comparing impact responses of the homogeneous and inhomogeneous human brain, in: *39th Stapp Car Crash Conf.*, Society of Automotive Engineers, 121-137.